이학석사 학위논문

The Role of Neuronal Growth Regulator 1 in Mouse Affective Discrimination via Regulating Adult Olfactory Neurogenesis

성체후각신경생성 조절을 통한 생쥐 정서식별에서 **NEGR1**의 역할

2023년 2월

서울대학교 대학원
뇌인지과학과 뇌인지과학전공

김 광 환

The Role of Neuronal Growth Regulator 1 in Mouse Affective Discrimination via Regulating Adult Olfactory Neurogenesis

Advisor: Sung Joong Lee, Ph.D.

Submitting a master's thesis of
Natural Science

December 2022

Graduate School of Natural Sciences
Seoul National University
Brain and Cognitive Sciences Major

Kwang Hwan Kim

Confirming the master's thesis written by
Kwang Hwan Kim
December 2022

Chair	이 인 아	(Seal)
Vice Chair	이 성 중	(Seal)
Examiner	LEE SANG AH	(Seal)

ABSTRACT

The Role of Neuronal Growth Regulator 1 in Mouse Affective Discrimination via Regulating Adult Olfactory Neurogenesis

Kwang Hwan Kim

Brain and Cognitive Sciences Major

Graduate School of Natural Sciences

Seoul National University

Sensory reactivity and affective recognition are impaired in patients with autism spectrum disorder (ASD). Affective information is transmitted as sensory inputs such as facial expression, tone of voice, and body odor. Considering the fact that ASD patients show atypical sensory vigilance, it is assumable that unregulated affective-sensory stimulus leads to impairment in affective recognition. However, no ASD mouse model co-manifesting these symptoms is available, thereby limiting the exploration of the relationship between affective recognition and sensory processing in ASD. Here I investigated the function of NEGR1, a recently-identified risk gene of ASD, in mouse affective discrimination and olfactory sensory processing using *Negr1*$^{-/-}$ mice. Upon encountering restraint stress or chronic pain demonstrator mice, *Negr1*$^{-/-}$ mice fail to distinguish them from neutral demonstrators, showing indifferent social investigation. Besides, although *Negr1*$^{-/-}$ mice can detect social odors, they showed aberrant olfactory habituation and dishabituation against social odors. In electrophysiological studies, inhibitory inputs to the mitral cells in the olfactory bulb (OB) were increased in *Negr1*$^{-/-}$ mice compared with wild-type mice, and subsequently their excitability was decreased. As a potential underlying mechanism, I found that adult neurogenesis in the posterior subventricular zone (SVZ) was impaired in *Negr1*$^{-/-}$ mice, which results in the reduction of newly generated inhibitory neurons in the OB. Taken together, this data reveals an unexpected correlational link between affective recognition and olfactory sensory processing modulated by NEGR1. I propose a novel neurobiological mechanism of autism-related behaviors based on disrupted adult olfactory neurogenesis.

Keyword: Neuronal growth regulator 1 (NEGR1); autism; affective discrimination; olfactory processing; adult olfactory neurogenesis

Student Number: 2020-22323

TABLE OF CONTENTS

LIST OF FIGURES

1. INTRODUCTION

1.1. Background

1.1.1. Sensory processing and socio-affective recognition in autism

Autism is characterized by atypical sensory processing and impaired sociability. To investigate the underlying neuropsychological features in respect of autism's sensory processing and sociability, researchers primarily focused on the visual processing on the facial stimulation in people with autism (Dalton et al., 2005; Davies et al., 2011). ASD children, for example, showed an atypical pattern of eye-movement when conversating with others in-person (Zhao et al., 2022). Moreover, despite of the case that ASD participants correctly gazed at the target area in social scenes, they could not recognize social oddities accurately (Benson et al., 2016). Together, autistic people are impaired in not only regulating sensory-motor reactions when running into social stimulation but also interpreting social stimuli even if they rightly notice the target (Hedley et al., 2012; Zhao et al., 2022). This socio-cognitive abnormality is closely related to atypical neural activation. When autistic participants were giving attention to emotional stimuli, social-related brain areas such as amygdala or fusiform gyrus were activated differently from control participants (Dalton et al., 2005; Deeley et al., 2007; Kleinhans et al., 2011; Sanders et al., 2022).

1.1.1.1. olfaction for socio-affective recognition

Although vision is regarded as the predominant sensory modality to recognize social stimulation purportedly, most animals mainly use olfaction to explore, identify, and interact with their conspecifics (Contestabile et al., 2021; Kristensen et al., 2001; Mateo, 2009). In human studies, people unconsciously noticed an intimate person by their body odors (Ravreby et al., 2022), aggressively reacted to a social chemosignal, or hexadecanal (Mishor et al., 2021), and showed amygdala activity when smelling emotional stress sweat (Mujica-Parodi et al., 2009). These findings suggest that socio-affective information is influenced by social chemosignals when people interact with others. Moreover, considering dysregulation in olfactory processing of patients with ASD (Rozenkrantz et al.,

2015; Sweigert et al., 2020), it is assumable that their impaired sociability is linked with abnormal olfactory function. Endevelt-Shapira et al. (2018), for instance, revealed that whereas typically-developed participants showed the increase in physiological arousal and reduction in measured social trust in response to smell of fear, which was gathered after sky-dive, ASD participants responded to the same smell in the opposite way. In conclusion, although it is counterintuitive that people utilize olfactory stimuli as socio-affective information, the findings above increasingly support the importance of investigating the role of olfaction in a social context.

1.1.1.2 Olfactory abnormality and social impairment in autism rodent model

Various autism rodent models, developed by adapting genetic and environmental modifications, have shown social impairment in a number of studies (Hörnberg et al., 2020; Lim et al., 2021; Peñagarikano et al., 2015; Peça et al., 2011; Reed et al., 2020). In those studies, the three-chamber social test (3CST) was mostly used to assess sociability and/or social novelty (Lim et al., 2021; Peñagarikano et al., 2015; Peça et al., 2011; Reed et al., 2020). In the test, autism model mice spent less investigating time other mice; they also showed diminished interaction time with a novel mouse when they simultaneously encountered a familiar and a novel mouse. This indicated that autism model mice were not interested in social interaction compared to normal mice (Lim et al., 2021; Peñagarikano et al., 2015) and could not discriminate between familiar and novel mice (Hörnberg et al., 2020).

Regarding olfactory abnormality, however, studies reported inconsistent results. Some autism rodent models showed olfactory dysfunction (Levy et al., 2019; Li et al., 2020; Nakamura et al., 2021); in contrast, other model mice were intact in their olfactory functions (Kwak et al., 2021; Wang et al., 2018). These discrepancies may be due in part to the cursory methods applied to study olfactory dysfunction, merely identifying the presence or absence of olfactory abnormalities. Olfactory function is composed of sub-skills such as detection, identification, and discrimination of olfactory stimuli; researchers should examine each skill separately to reveal olfactory dysfunction in more detail. For example, while autism patients were able to detect odors as much as normal participants did, they inaccurately identified odors (Galle et al., 2013; Sweigert et al., 2020) and reacted

to (un)pleasant odors as if they did not distinguish them (Rozenkrantz et al., 2015). Therefore, a systematic analysis of olfactory behaviors is required to clarify olfactory dysfunction in autism rodent models.

1.1.1.3 Affective recognition in rodent studies

It has been demonstrated that rodents behave in response to the conspecifics' affective states in experimental settings (Bartal et al., 2011; Jeon et al., 2010; Smith et al., 2021). When rodents notice their conspecifics are in stress or pain, they help out or mimic conspecifics' behaviors. This indicates that rodents recognize others' affective state and that affective behavior is contagious among rodents in a social context.

To investigate affective recognition and its neural underpinnings precisely, researchers employed the affective state discrimination test (ADT) while modulating neural activities with opto- or chemogenetics (Ferretti et al., 2019; Rogers-Carter et al., 2018; Scheggia et al., 2020). Notably, Scheggia et al. (2020) pointed out that emotional recognition can be studied by isolating it from general sociability, showing that inhibiting somatostatin interneurons in the medial prefrontal cortex (mPFC) altered social preference for emotional conspecifics during the ADT but did not influence mouse's sociability during the 3CST. Thus, ADT now allows researchers to investigate affective perception per se systematically. Yet, studies using ADT primarily focused on associative brain areas where affective information was in the middle of neural processing: mPFC (Scheggia et al., 2020), insular cortex (Rogers-Carter et al., 2018), and central amygdala (Ferretti et al., 2019). Given that affective information is initiated by sensory signals, then is integrated and processed via multiple brain areas, a study in respect of the sensory part of the process is needed to open the door to figure out the affective discrimination process as a whole.

1.1.2. Neuronal growth regulator 1 as an autism-relevant molecule

Neuronal growth regulator 1 (NEGR1), also named as Kilon, has been reported as an ASD candidate risk gene in animal and genome-wide associated studies (Grove et al., 2019; Singh et al., 2018b; Szczurkowska et al., 2018). In mouse studies, *Negr1*$^{-/-}$ mouse showed autistic-like behaviors – social impairment and repetitive behavior – implied by reduced time in a social chamber, less social

sniffing time, and increased self-grooming time (Singh et al., 2018; Szczurkowska et al., 2018).

NEGR1 is a glycosylphosphatidylinositol (GPI)-anchored cell adhesion molecule (CAM) and has three immunoglobulin (Ig)-like motifs in its extracellular domain (Funatsu et al., 1999) (Figure 1). With the structural characteristics, NEGR1 is classified as IgLON (Ig superfamily containing LAMP, OBCAM, and Ntm) with other GPI-anchored proteins that have three Ig-like motifs (Miyata et al., 2003). One mechanism of neuronal regulation by NEGR1 is that it forms a heterodimer with *cis* membrane proteins or acts as a ligand for *trans* membrane proteins, thereby transducing intracellular signals regulating transcriptions (Noh et al., 2019; Szczurkowska et al., 2018). Another mechanism is that the extracellular domain of NEGR1 is shed by a metalloproteinase, resulting in producing soluble NEGR1 that modulates neuronal growth (Pischedda & Piccoli, 2016; Sanz et al., 2015).

IgLONs basically have an effect on neurodevelopment, including synapse and neurite formation (Hashimoto et al., 2009; Jagomäe et al., 2021; Singh et al., 2018b). NEGR1, in particular, was reported as being associated with neurogenesis, neuronal migration, dendritic spine density, and axon elongation (Noh et al., 2019; Singh et al., 2018a; Szczurkowska et al., 2018). Given that studies using other autistic models targeting ASD risk genes such as *SHANK3*, *CACNA1C*, and *CNTNAP2* showed the neural alterations as described above, the NEGR1 is

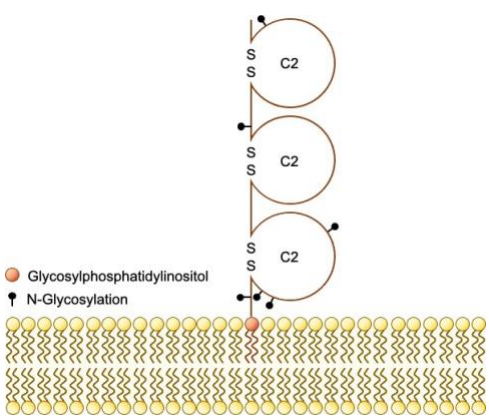

Figure 1. The Structure of NEGR1. NEGR1, the GPI-anchored protein, has three immunoglobulin-like C2-set domains. Black dots represent N-glycosylation attached to NEGR1.

considered to have the convergent neural attribute of autistic symptoms observed in other mouse models of autism (Bariselli et al., 2016; Birey et al., 2022; Kim et al., 2022; Peñagarikano et al., 2011; Wegscheid et al., 2021). Thus, it is expected that investigating the role of NEGR1 in neural maturation encourages may elucidate cardinal part of pathophysiological mechanism underlying autistic symptoms.

1.1.3. Olfactory neurogenesis and social behavior

Autism models are closely linked with olfactory neurogenesis in that neuronal proliferation, migration, and synaptic maturation take part in the process of olfactory neurogenesis. Newly generated olfactory neurons are continuously integrated into the olfactory bulb (OB) via the rostral migratory stream (RMS) in the rodent (Doetsch & Alvarez-Buylla, 1996; Lois & Alvarez-Buylla, 1994), primates (Kornack & Rakic, 2001; Wang et al., 2011), and potentially human's brain throughout life (Curtis et al., 2007; Sanai et al., 2011; Wang et al., 2011) (Figure 2). To be more precise, neuroblasts are generated from neural progenitor cells embedded in SVZ, then drift to OB along RMS, and are matured to become diverse subtypes of inhibitory neurons while positioning in the granule cell layer

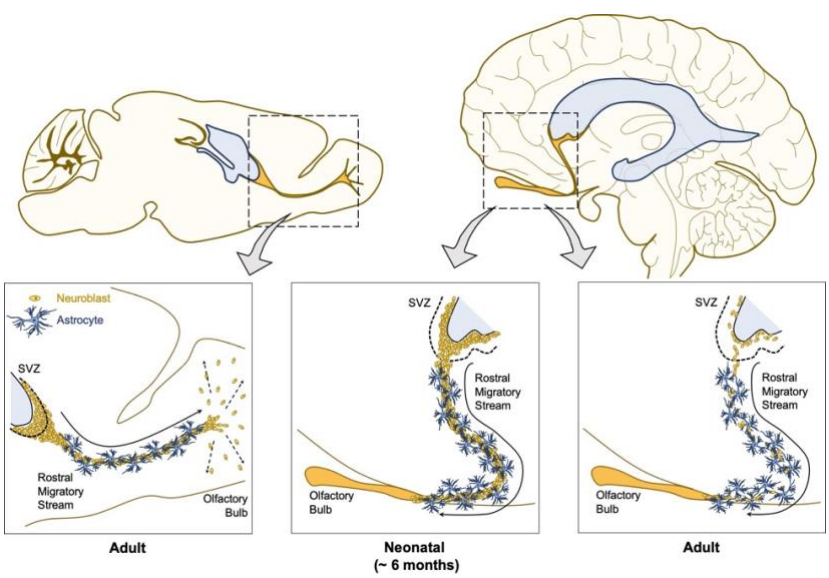

Figure 2. **The pathway between the subventricular zone and the olfactory bulb in the brains of the adult mouse, the neonatal and adult human.** Olfactory neurogenesis continues for entire life in the mouse brain, which, but, is limited during neonatal period in the human brain.

(GCL) or the glomerular layer (GL) (Merkle et al., 2007, 2014).

Olfactory neurogenesis plays a role in olfactory perceptual learning, including olfactory learning and odor discrimination (Gheusi et al., 2000; Grelat et al., 2018; Moreno et al., 2009; Shani-Narkiss et al., 2020). For example, when adult olfactory neurogenesis was disrupted by x-ray irradiation, the mice were impaired in maintaining odor-cued fear learning, but their basic olfactory functions, such as detection and acquisition, were intact (Valley et al., 2009). This suggests that olfactory adult neurogenesis is required for olfaction-mediated cognitive behaviors.

Notably, studies have shown that olfactory neurogenesis also affects social behaviors (Feierstein et al., 2010; Sakamoto et al., 2011). When newly generated olfactory neurons were under apoptosis for an extended period by diphtheria toxin fragment A, mice failed to show normal consummatory social behaviors such as aggressive, mating, and parental behaviors (Sakamoto et al., 2011). Besides, the increased olfactory neurogenesis by fluoxetine treatment rescued impaired social memory (Guarnieri et al., 2020). These findings suggest that olfactory neurogenesis is necessary and sufficient for sound social interaction.

1.2. Purpose of Research

Despite the fact that deficits in recognizing affective and sensory perception are concurrently manifested in ASD, the relationship between those two impairments in a mouse model of autism has not been thoroughly explored. Here, I tested both affective discrimination and diverse skills of olfactory function in *Negr1*$^{-/-}$ mice. Furthermore, I examined electrophysiological properties in the OB and adult olfactory neurogenesis to investigate putative neurobiological mechanism of the deficit in affective discrimination.

2. BODY

2.1. Methods

2.1.1. Animals

Negr1$^{-/-}$ mice of C57BL6/N background were genotyped by polymerase chain reaction (PCR) with the tip of the tail (Noh et al., 2019). C57BL6/N wild-type (WT) mice were purchased from DooYeol Biotech (Seoul, South Korea). Male mice were used in all experiments aged 9 to 15 weeks old. The animals were maintained in a temperature- and humidity-controlled room (20-23℃, 55% humidity) with 12 h light/dark cycles (light for 8 am to 8 pm, dark for 8 pm to 8 am). At least two mice were housed in each home cage, to avoid social isolation, and provided regular lab chow and water *ad libitum*. All animal care and experiments conformed to the guidelines provided by the Institutional Animal Care and Use Committee (IACUC) of Seoul National University.

2.1.2. Behavioral tests

All testing mice were handled for three days (5 min/day), one week before a test. Habituation and tests were performed between 12 pm to 6 pm to minimize circadian variation. The mice were placed inside the soundproof test room at least 30 min before all sessions. The light intensity of the test room was the same as the daylight of the animal room. For social-related tests, the home cages of observer mice were put in separate lines of the animal rack to keep them from prior exposure to social stimuli used in the experiments. Experimental apparatuses were cleaned with 70% ethanol after each experimental session.

2.1.2.1. Affective state discrimination test (ADT)

Habituation. The ADT was performed as previously described (Ferretti et al., 2019; Scheggia et al., 2020). Observer mice were habituated for three consecutive days before the test (10 min/day) in a cage the same size as their home cages (20 × 32 × 14.5 cm, Three-Shine Inc., Daejeon, South Korea). There was a black separator (11 × 14 cm) in the middle of the cage, and two cylindrical wire cups (18 cm in height, 7 cm diameter, 1 cm spaced bars) were placed in two corners of the cage's long side. The separator was set to prevent the demonstrator mice from seeing each

other, leaving space for the observer mouse to move freely between two demonstrator areas. On the same days, demonstrator mice that were matched by age to the observer mouse were habituated in the wire cup inside the experimental cage without the observer mouse (10 min/day).

Test. The observer mouse was placed inside the experimental cage with empty wire cups for 10 min before the test. Then, wire cups with demonstrators (one neutral and another stress- or pain-evoked) were replaced with empty cups, and the 6 min test was started. All experimental cages were used only once and replaced with an autoclaved cage to prevent the carryover effects due to remaining social odors. The neutral and affectively-evoked demonstrators were alternately placed in the two sides of the cage to counterbalance the spatial effect. All test trials were recorded by the camera on the top of the cage. Sniffing behavior was scored manually using videos by the experimenter who blinded to observer genotypes and demonstrator affective states.

Neutral demonstrator. Neutral mice were housed separately from affectively-evoked demonstrators to prevent them from affective contagion. As counterparts for stress demonstrators, neutral mice were maintained in their home cages without any manipulation. As counterparts for pain demonstrators, neutral mice underwent sham surgery. Before and after surgery, the von Frey test was performed to confirm whether the surgery evoked pain, and only mice who did not exhibit pain responses were used as neutral demonstrators.

Stress demonstrator. Stress was evoked by tube restraint. Stress demonstrators were restrained in the 50 ml tube with breathing holes for 15 min and then immediately moved to the experimental cage.

Pain demonstrator. The pain was evoked by sciatic nerve transection (SNT) surgery, as previously described (Lim et al., 2017) with minor modifications. Mice were anesthetized by 1.5 to 2% isoflurane with room air. We exposed approximate L4 to L6 vertebrae by incising the back skin. Under the stereo microscopic view, the right side of the L5 transverse process was removed with forceps and the L5 spinal nerve was transected. Then the incision was closed with surgical staples. For sham surgery, the mice underwent the same surgical procedure without the L5 nerve transection. The von Frey test was used to confirm pain before and after the surgery. The mice were represented as a demonstrator seven days after the surgery.

2.1.2.2. von Frey test

The von Frey test was performed to measure mechanical allodynia before and after SNT surgery, as previously described (Lim et al., 2017). One week before the test, animals were habituated in the transparent acryl chamber (4 × 8 × 4 cm) on an elevated wire grid (50 cm in height) for three days (2 h/day). On the test day, animals were habituated for 30 min in the test room to preclude a startle response. At the beginning of the test, the middle of the plantar surface on the right hind paw, ipsilateral to the transected nerve, was poked with the 0.6 g von Frey filament perpendicularly from below the grid. Variable weights of filaments (0.02 to 6 g, Stoelting, Wood Dale, IL, USA) were used and we increased or decreased the weights according to their pain responses: heavier filament after the absence of response, lighter filament after pain response. The pain response – withdrawing, flicking, or licking the paw – were scored by an experimenter blinded to the group assignment. Lastly, the scores were calculated with the up-down method (Chaplan et al., 1994).

2.1.2.3. Three chamber social test (3CST)

The tested mice were habituated in the rectangular acryl arena (63 × 45 × 30 cm) for three consecutive days before the test (10 min/day). The arena was divided into three chambers with doorways allowing a mouse in and out of each chamber, and wire cups, the same ones used in the ADT, were placed in the left and right chambers of the arena. Simultaneously, mice used as social stimuli were habituated in the wire cups. On the test day, the test mouse was put in the center chamber with the doors closed, then 10 min habituation started after the doors were opened. After the habituation, the doors were closed while the test mouse was in the central chamber, and a social stimulus was introduced in either the left or right chamber. The location of social stimulus alternated each session. Then, the doors were opened, and 10 min sociability test started. Finally, the doors were closed again while the testing mouse was in the middle chamber. A novel mouse was placed on the other side of the chamber, where an empty wire cup had been left, then 10 min social novelty test started. Each experiment was recorded by a camera on the top of the arena and analyzed with the automatic video tracking system (SMART 3.0; Panlab, Barcelona, Spain).

2.1.2.4 Sensory-controlled social interaction test

I performed sensory-controlled social interaction tests to examine the roles of different sensory stimuli during social interaction in the same experimental conditions as ADT. Cylindrical cups used in this test were designed as previously described (Contestabile et al., 2021) with minor modifications (all kinds of the cylindrical cup had the same size, 18 cm in height, 7 cm diameter): (1) black opaque with small openings (0.3 cm diameter), preventing visual cues but allowing olfactory cues; (2) transparent without openings, allowing visual cues but preventing olfactory cues; (3) black opaque without openings, preventing both visual and olfactory cues. This test followed the same experimental procedure as the ADT, but the observer mouse interacted with three unfamiliar conspecifics in different sensory-controlling cylindrical cups (3 days apart). For the visual-only cup, a non-social stimulus, a bowling pin toy, was presented on the other side of the cage. The order of the social stimulus presentation was counterbalanced to preclude the order effect. Behavior was recorded by a camera on the top of the cage, and sniffing was scored with the videos by an experimenter blinded to observer genotypes.

2.1.2.5. Buried Food test

The buried food test was performed in the same-sized cage as the home cage. Animals fasted for 24 hours before the test to motivate them to forage for food. An autoclaved cage and fresh bedding (3 cm depth) were used for each test. A mouse was first placed in a clean cage for habituation (5 min), then transferred into another clean cage where a pellet (3 ± 1 g) was buried beneath the bedding on the bottom, in the corner of the cage. The mouse was placed in the diagonally opposite corner from the food pellet. Behavior was recorded by a camera on the top of the cage and the recording was finished after the mouse found the food. The latency to finding food was measured by an experimenter blinded to mice genotypes.

2.1.2.6 Odor discrimination learning test

The odor discrimination learning test was performed as previously described (Imayoshi et al., 2008; Takahashi et al., 2016) with minor modifications. From the day before this experiment to the last day, food was restricted to maintaining mice's body weight at 80 to 85% of their free-feeding weight during the test to increase

the probability of reward association. The mice were trained in a cage with two types of monoterpenoid odor (S- and R-carvone, 6.4 M, 20 µl, Sigma-Aldrich, Burlington, MA, USA) alternately for four days. S-carvone was placed on the surface of the bedding with pieces of crystal sugar (Pastorale, Ile-de-France, France) for reward association, but R-carvone was left without the sugar; both odors were presented on a piece of laboratory wiper (26 × 26 mm; Yuhan Kimberly, Seoul, South Korea) in a multiperforated petri dish (35 mm). Tests were performed on mice (5 min/test). from the fifth to seventh days. On the fifth day, the mice were placed in a cage where two odors in the petri dish were buried under clean bedding (5 to 6 cm) it two opposite corners of the cage without sugar. On the sixth and seventh days, reward-associated S-carvone and neutral R-carvone odor was hidden under the bedding, respectively. When training and test took place on the same day, the training was conducted on the mice after the test. The behaviors were recorded by the camera on the top of the cage to measure digging and analyzed by an experimenter blinded to mouse genotypes.

2.1.2.7. Odor habituation and dishabituation test

Each mouse was habituated in an autoclaved cage with clean bedding for at least 40 min alone. A total of five odors were used during the test: water, banana extract (McCormick, Pope County, MD, USA), almond extract (McCormick), and two social odors gathered from unfamiliar cages. Each odor was presented three times to the test mouse on a cotton swab (20 µl), and every turn lasted for two minutes, followed by a one-minute break. The behavior was videotaped on the long side of the cage, and sniffing was scored by an experimenter blinded to mouse genotypes. Sniffing score was furtherly analyzed as previously described (Wesson et al., 2010). For odor habituation, sniffing time during each turn was normalized by the maximum sniffing time of each odor per mouse (e.g., normalized maximum sniffing = 1). The normalized scores were used again to assess odor dishabituation, in which the normalized habituation index of the last turn of each odor was subtracted from the following first normalized habituation index.

2.1.3. Bromodeoxyuridine (BrdU) incorporation assay

BrdU assays were used to identify cells generated after BrdU administration. BrdU was dissolved in saline (10 mg/ml) at 55℃ and intraperitoneally injected into

9-week-old mice four times every two hours for one day (50 ml/kg). The mice were sacrificed eight days after BrdU injections, since neuroblasts migrating from SVZ arrive at the outer layer of the OB, the glomerular layer (GL), six to seven days after the injection (Kovalchuk et al., 2015; Lois & Alvarez-Buylla, 1994).

2.1.4. Immunohistochemistry (IHC)

Mice were anesthetized with 20% urethane and perfused with 0.1 M phosphate-buffered saline (PBS), followed by 4% paraformaldehyde (PFA). Mouse brains were post-fixed overnight with PFA, then dehydrated in 30% sucrose for three days at 4℃. Brains were coronally sectioned at -21℃ with 40 μm thickness. The sections were blocked for 1 h at room temperature (RT) with a blocking solution (5% normal goat serum, 2% bovine serum albumin, 0.15% Triton X-100 diluted in PBS), then incubated for 21 to 24 h at RT with primary antibodies diluted in blocking solution. The sections were washed with PBS for 10 min three times to wash off the primary antibodies, then incubated with secondary antibodies in 1.5% normal donkey serum, 0.15% Triton X-100 diluted in PBS for 2 h. The following is the list of primary antibodies: anti-Ki67 (rat, 1:2000, Invitrogen, Waltham, MA, USA, 14-5698-80), anti-BrdU (mouse, 1:2000, Invitrogen, MA3-071), anti-GAD67 (rabbit, 1:2000, Invitrogen, PA5-21397), and of secondary antibodies: Cy3-, Cy5- and FITC-conjugated donkey IgG (1:200, Jackson Immunoresearch, West Grove, PA, USA, 712-165-150, 712-165-153, 715-175-150, 715-095-150). The sections were washed by PBS for 10 min three times, then mounted on coated glass slides with Vectashield (Vectashield Laboratory, Newark, CA, USA).

2.1.5. Image analysis

Brain sections were imaged on Zeiss LSM800 confocal microscope（Carl Zeiss Meditec, Thuringia, Germany). Image acquisition conditions were leveraged on a random slice of WT mice. OB (AP: +4.28 mm), anterior SVZ (AP: +1.62 mm), and posterior SVZ (AP: +0.74 mm) were selected as regions of interest to identify neural progenitors (Ki67-expressing) along the RMS. Three slices for each brain region were collected per mouse with identical gaps. All of the sections were imaged at 20× magnification. Ki67-expressing cells were manually counted with ImageJ (NIH, Bethesda, MD, USA). The mean of cell counts was used as a representative value for each mouse. OB slices were selected as a region of interest

to identify newly generated cells (BrdU-incorporated). For whole slice images, three sections were imaged per mouse at 20× magnification. The counts of BrdU-incorporated cells were averaged within layers of the OB per each mouse to obtain a representative value. For z-stacked images (63× magnification, 1 μm step size), four fields of view were randomly selected in the GCL and GL, respectively, and the cell counts were averaged within each layer per mouse. Co-stained glutamic acid decarboxylase 67 (GAD67) was used to confirm whether BrdU-incorporated cells were inhibitory cells.

2.1.6. Whole-cell voltage-clamp

Transverse acute slices of the olfactory bulb (300 μm) were prepared. Briefly, mice were anesthetized with isoflurane and decapitated. The brain was rapidly removed and placed in ice-cold oxygenated (95% O_2 and 5% CO_2), low-Ca^{2+}/high-Mg^{2+} dissection buffer containing 5 mM KCl, 1.23 mM NaH_2PO_4, 26 mM $NaHCO_3$, 10 mM dextrose, 0.5 mM $CaCl_2$, 10 mM $MgCl_2$, and 212.7 mM sucrose. Slices were transferred to a holding chamber in an incubator containing oxygenated (95% O_2 and 5% CO_2) artificial cerebrospinal fluid (ACSF) composed of 124 mM NaCl, 5 mM KCl, 1.23 mM NaH_2PO_4, 26 mM $NaHCO_3$, 10 mM dextrose, 2.5 mM $CaCl_2$, and 1.5 mM $MgCl_2$ at 28°C–30°C for at least 1 h before recording. After recovery, slices were transferred to the recording chamber where they were perfused continuously with ACSF gassed with 95% O_2/5% CO_2 at a flow rate of 2 ml/min. Slices were equilibrated for 5 min prior to recordings and all the experiments were performed at 30°C–32°C. Recordings were obtained using a Multiclamp 700B amplifier (Molecular Devices, Sunnyvale, CA, USA) under visual control with differential interference contrast illumination on an upright microscope (BX51WI; Olympus). Patch pipettes (4–6 MΩ) were filled with 135 mM K-gluconate, 8 mM NaCl, 10 mM HEPES, 2 mM ATP-Na, and 0.2 mM GTP-Na to record sEPSCs in voltage-clamp mode or neuronal excitability in current-clamp mode (pH 7.4 and 280–290 mOsm). Patch pipettes were filled with 130 mM CsCl, 1.1 mM EGTA, 2 mM $MgCl_2$, 0.1 mM $CaCl_2$, 10 mM NaCl, 10 mM HEPES, and 2 mM ATP-Na to record sIPSCs (pH 7.4 and 280–290 mOsm). Only cells with access resistance <20 MΩ and input resistance >100 MΩ were studied. The extracellular recording solution consisted of ACSF supplemented with picrotoxin

(100 μM) for sEPSC and excitability. The sIPSC was recorded with extracellular solution ACSF at 0 mV. Data were acquired and analyzed using pClamp 10.5 (Molecular Devices). Signals were filtered at 2 kHz and digitized at 10 kHz using Digidata 1550A (Axon Instruments, Union City, CA, USA).

2.1.7. K-means clustering

I applied K-means clustering to confirm *Negr1*$^{-/-}$ and WT mice are distinctively categorized according to behavioral features: the odor habituation, odor dishabituation, the first stage of affective discrimination, and the total of affective discrimination. We chose two centroids for the clustering based on both the prior knowledge that we used two genotypes of mice. The individual points within clusters were represented on the x-y plane after the applying dimensionality reduction principal component analysis (PCA). K-means clustering was performed using R studio.

2.1.8. Statistics

Data were presented as mean ± s.e.m. unless otherwise noted. Before group comparisons, the normality of distribution and the equality of variance were examined with the Shapiro-Wilk test and Levene's test, respectively. The *t*-test or Wilcoxon signed-rank test were used for two-group comparisons. Two-way mixed ANOVA with post hoc test, adjusted by Bonferroni correction, was used when more than two conditions were assigned to each group. Details are described for each experiment in the corresponding figure legend.

2.2. Results

2.2.1. *Negr1*$^{-/-}$ mice are impaired in affective discrimination for stress and pain

I employed ADT to examine the capability of *Negr1*$^{-/-}$ mice to discriminate the affective states of conspecifics (Figure 3a, 4a). Before the test, I measured locomotion and spatial bias during the habituation phase to exclude their confounding effects on affective discrimination. Neither WT nor *Negr1*$^{-/-}$ mice showed spatial bias, and *Negr1*$^{-/-}$ mice exhibited normal locomotion in the experimental cage (Figure 3b, 4b). After the habituation, I simultaneously presented stress-evoked and affectively-neutral mice (demonstrator) as social stimuli in the test cage. The WT observers investigated the stress-evoked demonstrator more than the affectively-neutral demonstrator in the test. Their preferential social investigations were noticeable in the first and the second two-minute durations (Figure 3d). However, the preference for the stress-evoked conspecifics was significantly attenuated in the *Negr1*$^{-/-}$ mice, indicating impaired discrimination (Figure 3c, d). To determine whether *Negr1*$^{-/-}$ mice are able to discern pain in conspecifics, I presented pain-evoked demonstrators to *Negr1*$^{-/-}$ mice (Figure 4a, 5a). For this, I employed a sciatic nerve transection (SNT) model, which causes mice to suffer from chronic neuropathic pain (Lim et al., 2017). I performed SNT and sham surgery on pain- and neutral-demonstrators, respectively (Figure 5a), and confirmed the pain induction with the von Frey test before and after the surgery (Figure 5b). Seven days after the surgery, I presented pain-evoked and affectively-neutral demonstrators to the ADT (Figure 4a). This time, WT mice preferred neutral mice over pain-evoked demonstrators with significant social preference in the first and the second two-minute durations. However, *Negr1*$^{-/-}$ mice did not show a social preference for either neutral- or pain-evoked demonstrators (Figure 4c, d). These data indicate that *Negr1*$^{-/-}$ mice are impaired in discriminating affective states among conspecifics.

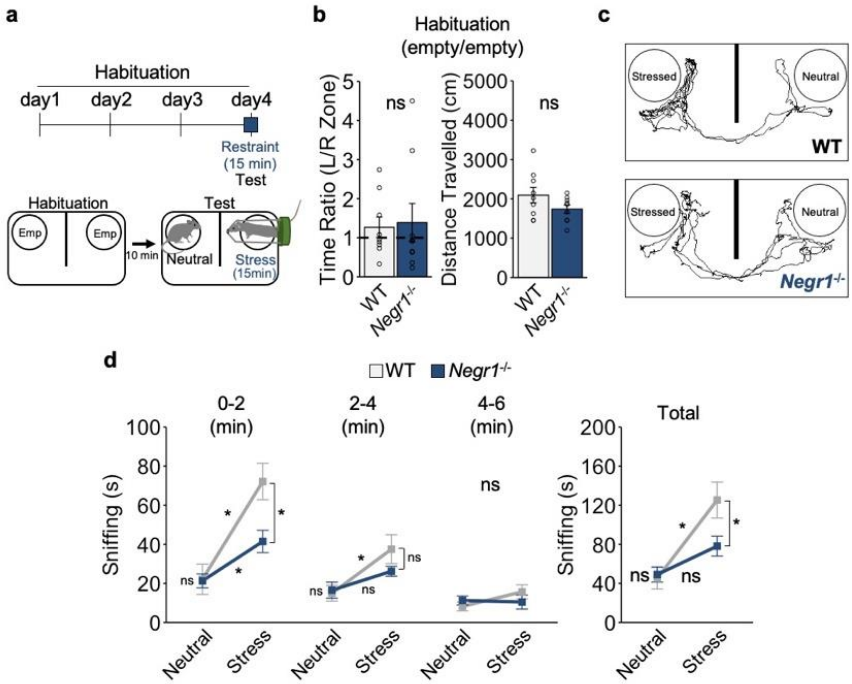

Figure 3. *Negr1*$^{-/-}$ mice are impaired in affective discrimination for stress.

a, The schematic design of emotional discrimination test for stressful/neutral (WT, n = 9; *Negr1*$^{-/-}$, n = 9). **b**, Left, time ratio between the right and left social areas (student's *t*-test, $P = 0.132$). Right, total distance traveled in the test chamber (one sample t-test, μ = 1, WT, $P = 0.336$; *Negr1*$^{-/-}$, $P = 0.448$). **c**, The moving traces during the early phase (0–2 min) of test. **d**, Left, the total 6 min of the test with stress/neutral demonstrators is divided into three sessions (each of 2 minutes), the first 2 min (left; two-way mixed ANOVA, interaction $F_{1,16} = 2.776$, $P = 0.115$; Bonferroni post hoc test, *$P < 0.05$), the second 2 min (middle; two-way mixed ANOVA, interaction $F_{1,16} = 1.768$, $P = 0.202$; Bonferroni post hoc test, *$P < 0.05$), and the last 2 min (right; two-way mixed ANOVA, interaction $F_{1,16} = 1.634$, $P = 0.219$). Right, during the total of six minutes (two-way mixed ANOVA, interaction $F_{1,16} = 2.768$, $P = 0.116$; Bonferroni post hoc test, *$P < 0.05$).

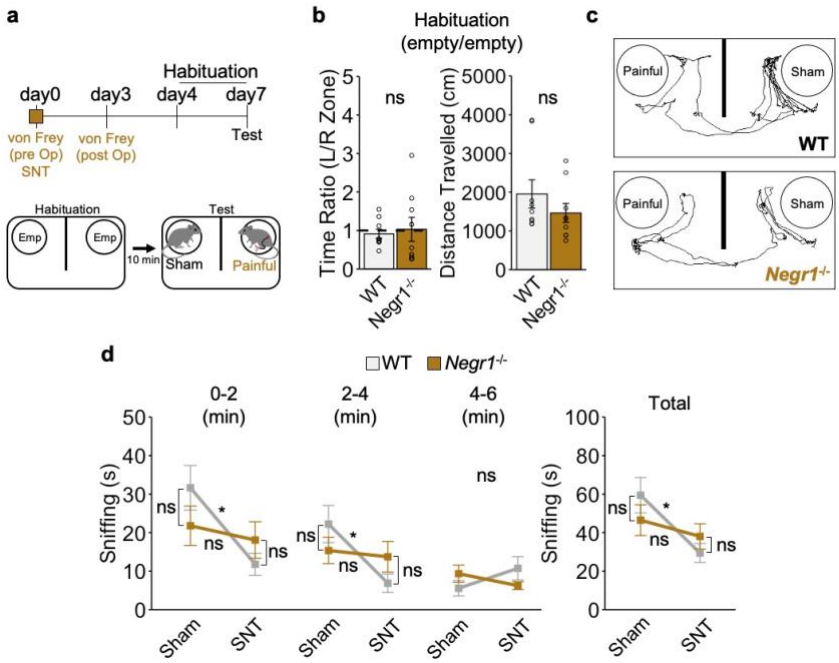

Figure 4. *Negr1*$^{-/-}$ mice are impaired in affective discrimination for pain.

a, The schematic design of emotional discrimination test for painful/neutral demonstrators (WT, n = 9; *Negr1*$^{-/-}$, n = 9). **b**, Left, time ratio between the right and left social areas (Wilcoxon signed-rank test, P = 0.258). Right, total distance traveled in the test chamber (one sample t-test, μ = 1, WT, P = 0.477; *Negr1*$^{-/-}$, P = 0.925). **c**, The moving traces during the early phase (0–2 min) of test. **d**, Left, the total 6 min of the test with painful/neutral demonstrators is divided into three sessions (each of 2 minutes), the first 2 min (left; two-way mixed ANOVA, interaction $F_{1,16}$ = 1.701, P = 0.211; Bonferroni post hoc test, *P < 0.05), the second 2 min (middle; two-way mixed ANOVA, interaction $F_{1,16}$ = 1.701, P = 0.151; Bonferroni post hoc test, *P < 0.05), and the last 2 min (right; two-way mixed ANOVA, interaction $F_{1,16}$ = 3.494, P = 0.080). Right, during the total of six minutes (two-way mixed ANOVA, interaction $F_{1,16}$ = 1.439, P = 0.248; Bonferroni post hoc test, *P < 0.05).

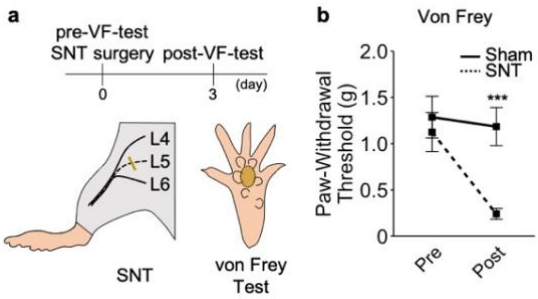

Figure 5. Sciatic nerve transaction induces neuropathic pain.

a, The schematic designs of SNT surgery and von Frey test (Sham, n = 18; SNT, n = 18). **b**, The paw-withdrawal threshold during the von Frey test (two-way mixed ANOVA, interaction $F_{1,34} = 7.329$; Bonferroni post hoc test, ***$P < 0.001$).

To determine whether NEGR1 is involved in other social-related behaviors, I assessed the sociability and social novelty of *Negr1*$^{-/-}$ mice using the three-chamber social test (Figure 6a). Before the test, I measured locomotion and spatial bias during the habituation phase to exclude their confounding effects. Neither WT and *Negr1*$^{-/-}$ mice showed spatial bias, and *Negr1*$^{-/-}$ mice had normal locomotion in the experimental apparatus (Figure 6b). Similar to WT mice, *Negr1*$^{-/-}$ mice preferred social stimuli over non-social stimuli interacting with conspecific mice as much as WT mice in the sociability testing phase (Figure 6c). However, interestingly, they were slightly impaired in recognizing novel conspecifics in the social novelty phase, though it was not statistically significant (Figure 6c, d). Taken together, although *Negr1*$^{-/-}$ mice showed normal sociability upon encountering social stimulation, they have difficulty in discriminating different social stimuli and affective states of conspecifics.

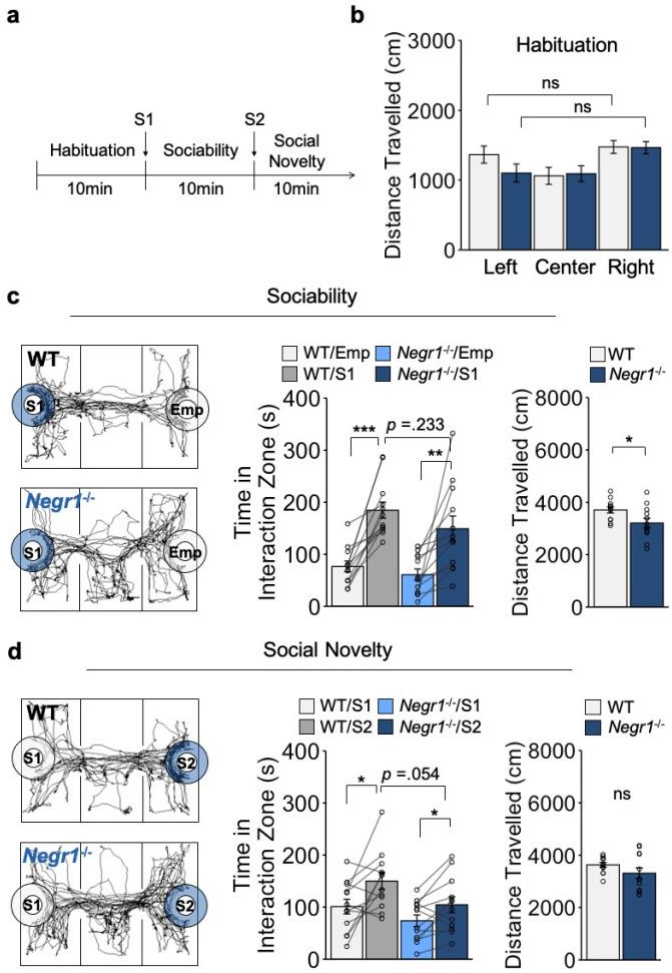

Figure 6. *Negr1*$^{-/-}$ mice are partially impaired in social novelty, but not sociability. **a**, The schematic design of the three-chamber social test (WT, n = 12; *Negr1*$^{-/-}$, n = 12). **b**, Traveled distance during the habituation phase (Bonferroni-corrected paired t-test, WT, adjusted $P_{\text{left-right}} = 1$; *Negr1*$^{-/-}$, adjusted $P_{\text{left-right}} = 0.801$). **c**, Left, the moving traces during the sociability phase. Middle, time in the interaction zone during the sociability test phase (two-way mixed ANOVA, interaction $F_{1,22} = 0.398$, $P = 0.535$; Bonferroni post hoc test, $^{**}P < 0.01$, $^{***}P < 0.001$). Right, traveled distance during the sociability phase (student's *t*-test, $^{*}P = 0.030$). **d**, The moving traces during the sociability phase. Middle, time in the interaction zone during the social novelty test phase (two-way mixed ANOVA, interaction $F_{1,22} = 0.716$, $P = 0.407$; Bonferroni post hoc test, $^{*}P < 0.05$). Right, traveled distance during the sociability phase (Welch's *t*-test, $P = 0.174$).

2.2.2. Dysregulated olfactory function of *Negr1*$^{-/-}$ mouse.

Affective and social recognition among rodents is mediated by sensory stimulation, such as visual detection of facial expression and olfactory detection of social chemicals (Contestabile et al., 2021; Dolensek et al., 2020; Ferretti et al., 2019; Langford et al., 2010). To identify the types of sensory modality involved in ADT, I adopted sensory-controlling acryl cups used to differentiate the effects of each sensory modality in a social test (Figure 7a) (Contestabile et al., 2021). While both *Negr1*$^{-/-}$ and WT mice were able to discern and investigate social stimulation in the olfactory cue-only acryl cups in which visual cues were blocked (Figure 7b, c), they did not discriminate conspecific vs. object without olfactory cues (visual cue only or non-visual & non-olfactory cues) (Figure 7b). These data indicate both WT and *Negr1*$^{-/-}$ mice primarily utilize their olfactory function for social recognition (Figure 7b, c). To further characterize the olfactory processing of social odors in *Negr1*$^{-/-}$ mice, I performed the odor habituation and dishabituation test by sequentially presenting social and non-social odors to the mice (Figure 8a). WT mice showed odor habituation and dishabituation by repeated exposure to both social and non-social odors (Figure 8b). However, *Negr1*$^{-/-}$ mice were impaired in habituation and dishabituation to social odors, but not non-social odors (Figure 8c, d), indicating *Negr1*$^{-/-}$ mice have aberrant olfactory processing specifically for social odors. Along with the impairment in olfactory processing of social odors, *Negr1*$^{-/-}$ mice showed a less sniffing behavior when exposed to non-social odors during the first trial (Figure 8e).

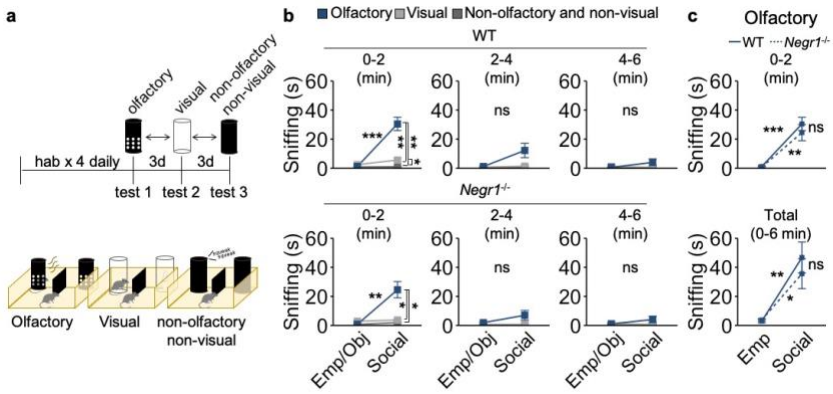

Figure 7. *Negr1*$^{-/-}$ mouse socially interacts with conspecifics via olfaction.

a, The schematic design of the sensory-controlled social test (WT, n = 8; *Negr1*$^{-/-}$, n = 7). **b**, Sniffing time during the sensory-controlled social test divided into three sessions (each 2 min; upper: WT, bottom: *Negr1*$^{-/-}$). Left, the first 2 min (two-way RM ANOVA; WT, interaction $F_{2,14} = 27.6$, $P < 0.0001$; *Negr1*$^{-/-}$, interaction $F_{1.07,6.42} = 16.2$, $P = 0.006$; Bonferroni post hoc test, *$P < 0.05$, **$P < 0.01$, ***$P < 0.001$). Middle, the second 2 min (two-way RM ANOVA; WT, interaction $F_{1.03,7.19} = 3.70$, $P = 0.094$; *Negr1*$^{-/-}$, interaction $F_{1.04,6.42} = 2.61$, $P = 0.156$). Right, the last 2 min (two-way RM ANOVA; WT, interaction $F_{1.03,7.18} = 2.18$, $P = 0.183$; *Negr1*$^{-/-}$, interaction $F_{1.09,6.52} = 1.88$, $P = 0.218$). **c**, Sniffing time for the olfaction-only condition for the comparison between WT and *Negr1*$^{-/-}$. Top, 0-2 min (two-way mixed ANOVA, interaction $F_{1,13} = 0.315$, $P = 0.584$; Bonferroni post hoc test, **$P < 0.01$, ***$P < 0.001$). Bottom: total 6 min (two-way mixed ANOVA, interaction $F_{1,13} = 0.381$, $P = 0.548$; Bonferroni post hoc test, **$P < 0.01$, ***$P < 0.001$).

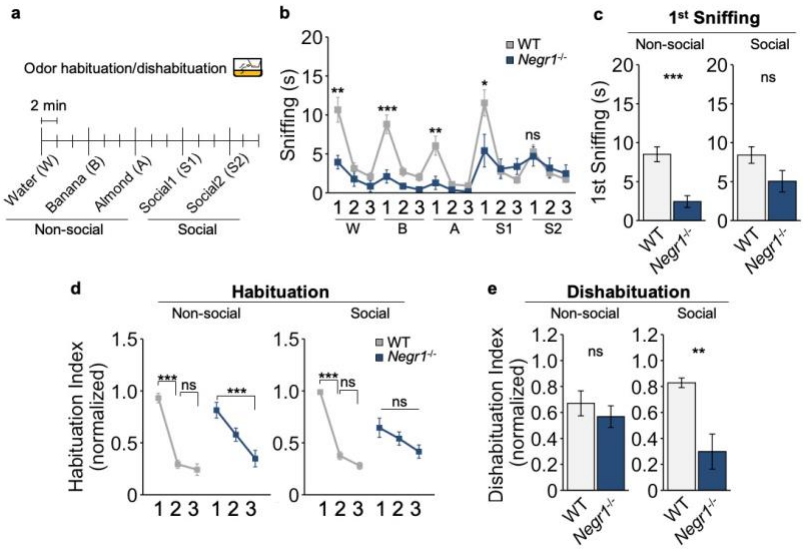

Figure 8. *Negr1*$^{-/-}$ mouse shows aberrant olfactory habituation and dishabituation for social odors.

a, The schematic design of odor habituation-dishabituation test (WT, n = 13; *Negr1*$^{-/-}$, n = 11). **b**, Raw sniffing time during the test (two-way mixed ANOVA, interaction $F_{14,308}$ = 4.787, P < 0.0001, Bonferroni post hoc test, *P < 0.05, **P < 0.01, ***P < 0.001). **c**. First sniffing time for non-social odors (left; Wilcoxon signed-rank test, ***P < 0.0003), for social odors (right; student's t-test, P = 0.063). **d**, Normalized olfactory habituation index for non-social odors (left, two-way mixed ANOVA, interaction $F_{2,44}$ = 5.310, P = 0.009; Bonferroni post hoc test, ***P < 0.001), for social odors (right; two-way mixed ANOVA, interaction $F_{2,44}$ = 12.377, P = 0.0005, Bonferroni post hoc test, ***P < 0.001). **e**, Dishabituation index for non-social odors (left; Wilcoxon signed-rank test, P = 0.147), for social odors (right; Welch's t-test, P < 0.003). Habituation index = sniffing/max(sniffing) in each session, dishabituation index = following 1st normalized habituation index – preceding 3rd normalized habituation index.

To confirm that the olfactory function for non-social odors is intact in *Negr1*$^{-/-}$ mice, I tested the ability of *Negr1*$^{-/-}$ mice to detect non-social odor by a buried food test (Figure 9a). *Negr1*$^{-/-}$ mice foraged hidden food as fast as WT mice by olfaction (Figure 9b), suggesting *Negr1*$^{-/-}$ detected non-social odors as efficiently as WT mice. Therefore, I hypothesized that although *Negr1*$^{-/-}$ mice had intact ability to detect social odors, they did not process social odors normally. As the odor-reward association accounts for the odor discrimination (Grelat et al., 2018; Pool et al., 2014), I tested whether *Negr1*$^{-/-}$ mice have impaired odor-reward associations by the odor discrimination learning test (Figure 10a). I trained both *Negr1*$^{-/-}$ and WT mice for four days to selectively associate S-carvone with rewards, crystal sugar, while R-carvone was not associated with the rewards. On the fifth day, after burying S- and R-carvone under the bedding, we tested whether mice showed preferential foraging behavior (i.e., digging) for the reward-associated odor, S-carvone, rather than the neutral odor, R-carvone. I found that *Negr1*$^{-/-}$ mice did not show preferences for S-carvone, indicating that they failed to discriminate between the reward-associated and the neutral odor (Figure 10b). Since *Negr1*$^{-/-}$ mice displayed aberrant olfactory habituation and dishabituation (Figure 8), it was unclear whether they failed to discriminate these two given odors or impaired in learning the rewarding value of S-carvone. To address this issue, we tested if *Negr1*$^{-/-}$mice successfully associated S-carvone with reward by presenting only S-carvone on the sixth day. Interestingly, while WT mice dug the S-carvone side preferentially over empty side, *Negr1*$^{-/-}$ mice did not dig bedding on the S-carvone-buried side (Figure 10b). These data indicate that *Negr1*$^{-/-}$ mice are impaired in associating odor with reward.

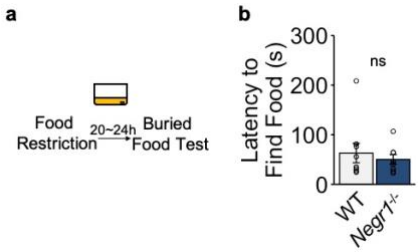

Figure 9. *Negr1*$^{-/-}$ mouse normally detects non-social odor.

a, The schematic design of the buried food test (WT, n = 9; *Negr1*$^{-/-}$, n = 8). **b**, Latency time to find food (Wilcoxon signed-rank test, P = 0.963).

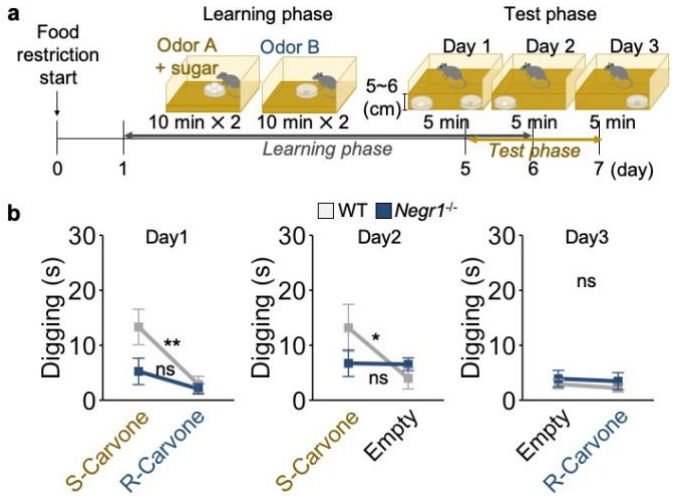

Figure 10. *Negr1*$^{-/-}$ mouse failed to associate a novel odor with reward.

a, The schematic design of the odor discrimination learning test (WT, n = 8; *Negr1*$^{-/-}$, n = 8). **b**, Digging time for the area under which odors are buried. Left, the first-day test for odor discrimination (two-way mixed ANOVA, interaction $F_{1,14}$ = 5.740, P = 0.031; Bonferroni post hoc test, **P < 0.01). Middle, the second-day test for reward-odor association (two-way mixed ANOVA, interaction $F_{1,14}$ = 7.309, P = 0.017; Bonferroni post hoc test, *P < 0.05). Right, the last-day test with the neutral odor (two-way mixed ANOVA, interaction $F_{1,14}$ = 0.043, P = 0.839).

Then, I conducted both odor habituation/dishabituation test and ADT in each mouse to test whether impaired affective discrimination is associated with social odor habituation and dishabituation (Figure 11a). Once again, social-odor habituation, dishabituation (Figure 11b, c) and social discrimination (Figure 11d, e) were significantly reduced in *Negr1*$^{-/-}$ mice. In these mice, affective discrimination is positively correlated with odor dishabituation during the early stage (0-2 min) and the total duration of the test (Figure 11d, e). In the correlation plot between odor dishabituation and affective discrimination (Figure 11d, e), *Negr1*$^{-/-}$ mice were plotted mostly on the left bottom, while WT mice were on the right top of the graph. This indicated that two groups were distinguished by olfactory dishabituation and affective discrimination features. I confirmed this finding by k-means clustering analysis, an unsupervised machine learning algorithm. In this analysis, *Negr1*$^{-/-}$ mice were distinctively categorized by odor (dis)habituation and affective discrimination measures (Figure 11f, g). These data demonstrate that affective discrimination and odor (dis)habituation are not only associated with each other but specify *Negr1*$^{-/-}$ is the atypical group.

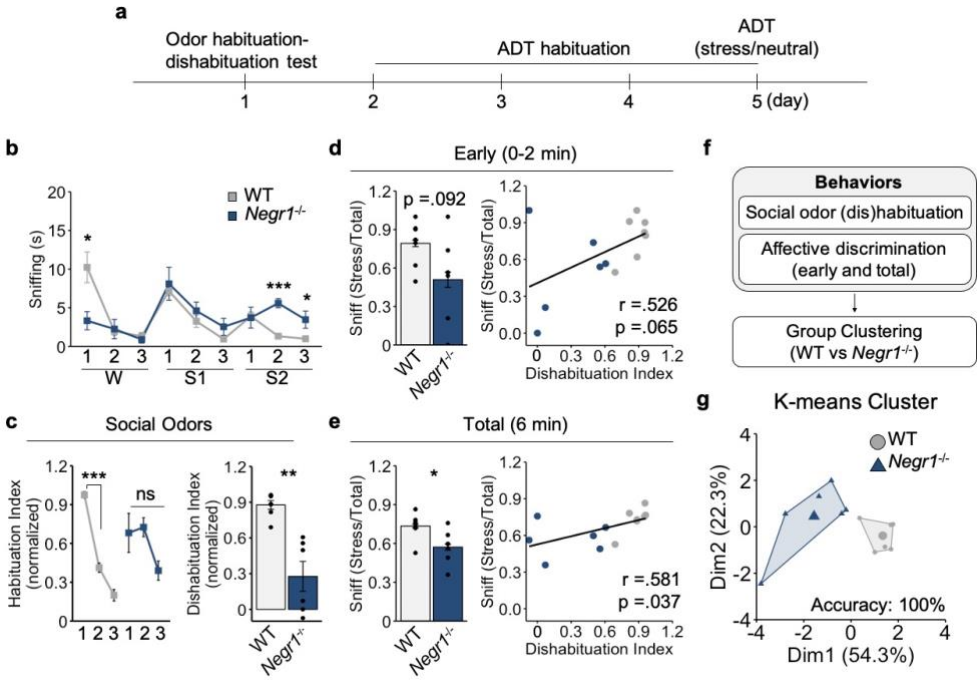

Figure 11. *Negr1*$^{-/-}$ mice are clustered distinctly from WT mice with olfactory (dis)habituation and affective discrimination.

a, The schematic design of the experimental schedule (WT, n = 7; *Negr1*$^{-/-}$, n = 6). **b**, Raw sniffing time during the odor habituation-dishabituation test (two-way mixed ANOVA, interaction $F_{8,88}$ = 5.318, P < 0.0001, Bonferroni post hoc test, *P < 0.05, ***P < 0.001). **c**, Left, olfactory habituation index for social odors (two-way mixed ANOVA, interaction $F_{2,22}$ = 8.603, P = 0.008; Bonferroni post hoc test, ***P < 0.001), Right, olfactory dishabituation index for social odors (Welch's t-test, **P = 0.004). **d,e**, The ADT in the early stage and in the total duration. Left, the sniffing ratio for the stress demonstrator (student's t-test, early, P = 0.092; total, *P = 0.034). Right, scatter plot with olfactory dishabituation index for the x-axis and sniffing ratio for the y-axis (Pearson correlation, early versus sniff, r = 0.526, P = 0.065; total versus sniff, r = 0.512, P = 0.037). **f**, The input behavioral measures used for k-means clustering. **g**, The scatter plot representing clusters on the x-y plane of the reduced dimensionality by the principal component analysis. Enlarged plots indicate the computed means of each group.

2.2.3. Inhibitory inputs in the mitral cells of *Negr1*$^{-/-}$ mouse were increased along with their decreased excitability

The findings indicated that *Negr1*$^{-/-}$ mice were impaired in social odor-processing functions. Odor information, such as value and identity, is represented by the mitral cell activities (Doucette et al., 2011; Gire et al., 2013; Wang et al., 2019; Xu et al., 2021), which are also involved in social recognition (Oettl et al., 2016) and social learning (Liu et al., 2017). Accordingly, to explore the functional alterations in mitral cells of *Negr1*$^{-/-}$ mouse, I performed whole-cell recordings of mitral cells in acute OB slices and recorded the spontaneous excitatory and inhibitory post-synaptic currents (sEPSCs and sIPSCs) and excitability (Figure 12a). Although I did not observe sEPSC changes (Figure 12b), sIPSCs were more frequently transmitted to mitral cells of *Negr1*$^{-/-}$ mice (Figure 12c) implicating an altered balance of excitatory and inhibitory synaptic transmissions (E/I balance) in mitral cells of *Negr1*$^{-/-}$ mice. In addition, the excitability of mitral cells was significantly decreased in *Negr1*$^{-/-}$ mice (Figure 12d). These data indicate that mitral cells of *Negr1*$^{-/-}$ mice are under decreased E/I ratio, and subsequently their action potentials being suppressed.

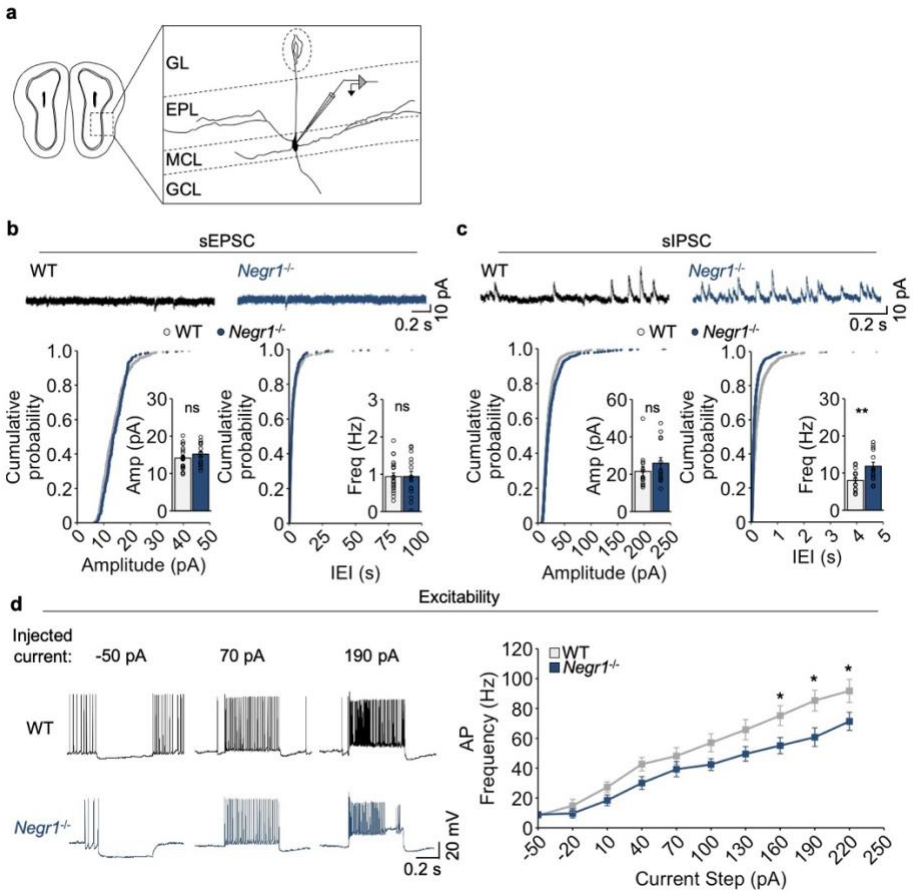

Figure 12. Inhibitory inputs are increased in the mitral cells of *Negr1*$^{-/-}$ mouse with a decrease in their excitability.

a, The schematic design of the whole-cell recording experiment. **b**, Representative current traces and quantified graphs of sEPSC. Left, amplitude (WT, n = 20 neurons, 3 animals; *Negr1*$^{-/-}$, n = 15 neurons, 3 animals; student's *t*-test, $P = 0.308$), Right, frequency (WT, n = 14 neurons, 2 animals, *Negr1*$^{-/-}$, n = 14 neurons, 2 animals; student's *t*-test, $P = 0.983$). **c**, Representative current traces and quantified graphs of sIPSC. Left, amplitude (Wilcoxon signed-rank test, $P = 0.352$), Right, frequency (student's *t*-test, $^{**}P = 0.008$). **d**, Representative voltage traces and quantified graphs of excitability (WT, n = 18 neurons, 3 animals; *Negr1*$^{-/-}$, n = 12 neurons 2 animals; two-way mixed ANOVA, $F_{9,288} = 2.526$, $P = 0.008$, Bonferroni post hoc test, $^{*}P < 0.05$).

2.2.4. The number of neural progenitor cells are reduced in *Negr1*$^{-/-}$ mouse.

It was previously reported that NEGR1 is required for adult hippocampal neurogenesis (Noh et al., 2019). Considering that adult olfactory neurogenesis affected olfactory discrimination (Shani-Narkiss et al., 2020), reward association (Grelat et al., 2018), and social recognition (Guarnieri et al., 2020), I determined whether impaired olfactory neurogenesis in *Negr1*$^{-/-}$ mice underlies the neural mechanism of olfactory dysfunction and impaired affective discrimination. I measured neural progenitor cells (NPCs) in SVZ, where adult olfactory neurogenesis begins, and in the OB, the final destination of olfactory progenitor cells (Figure 13a). The number of Ki67^{+} NPC was significantly reduced in the posterior part of SVZ (pSVZ), but not in the anterior part of SVZ (aSVZ) or in the OB, of *Negr1*$^{-/-}$ mice compared with WT mice (Figure 13b, c), indicating adult neurogenesis of *Negr1*$^{-/-}$ mice is impaired in a particular region of the SVZ.

Olfactory neurogenesis is spatially patterned between the SVZ and the OB (Merkle et al., 2007, 2014). Thus, I performed the BrdU incorporation assay to measure the number and the location of newly generated neurons in the OB eight days after BrdU administration (Figure 14a). I chose the GCL and GL as regions of interest since newly generated olfactory neurons are integrated in these layers (Merkle et al., 2007) (Figure 14e, f, and 15a). Compared with WT mice, the number of newly generated inhibitory cells (BrdU^{+} and GAD67^{+}) was decreased in the GL, but not in the GCL, of *Negr1*$^{-/-}$ mice (Figure 14g, h, and 15b). Taken together, these data indicate that adult SVZ neurogenesis and subsequent integration of new neurons into the GCL are reduced in *Negr1*$^{-/-}$ mice, which might contribute to aberrant olfactory processing and impaired affective discrimination.

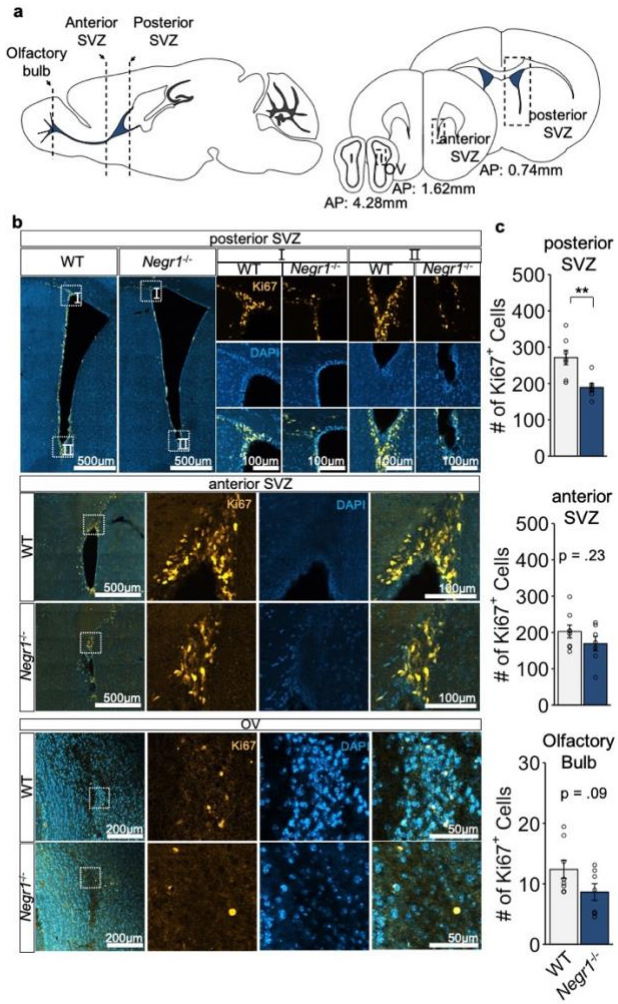

Figure 13. The number of pSVZ NPCs is reduced in *Negr1*$^{-/-}$ mouse.

a, Along the rostral migratory pathway, posterior subventricular zone (pSVZ), anterior SVZ (aSVZ), and olfactory bulb (OB) were chosen (WT, n = 8; *Negr1*$^{-/-}$, n = 7). Dashed lines on the brain saggital image indicate collected sections, and dashed line squares show regions of interest. **b**, Immunostaining showing Ki67 (organge) in pSVZ (top; scale bar, 500 μm, 100 μm), aSVZ (middle; scale bar, 500 μm, 100 μm), and OB (bottom; scale bar, 200 μm, 50 μm). White dashed line squares are magnified on the right side of the images. **c**, The number of Ki67^{+} cells in **b**, pSVZ (top; student's *t*-test, $^{**}P = 0.005$), aSVZ (middle; student's *t*-test, $P = 0.227$), and OB (bottom; student's *t*-test, $P = 0.915$).

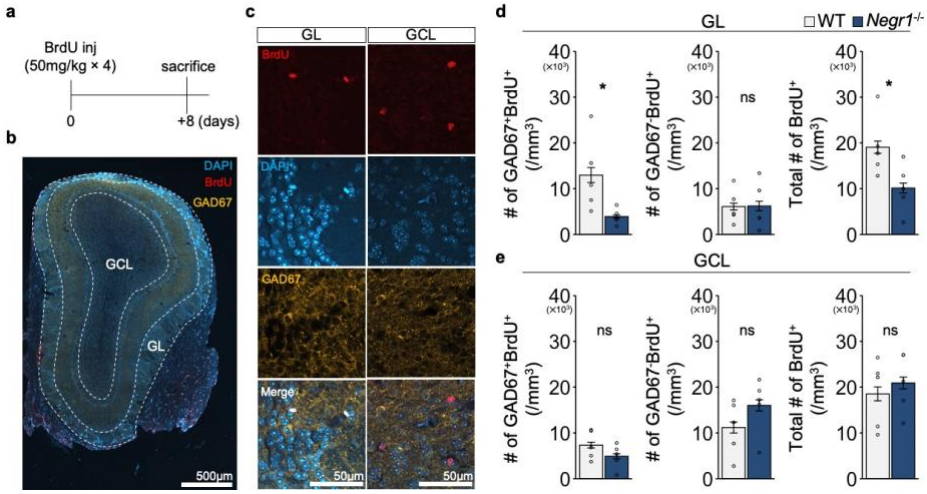

Figure 14. The number of newly generated inhibitory neurons is reduced in the GL of *Negr1*$^{-/-}$ mouse.

a, The schematic design of bromodeoxyuridine (BrdU) incorporation assay. **b**, The whole image of olfactory bulb delineating granule cell layer (GCL) and glomerular layer (GL). Scale bar, 500 μm. **c**, Representative immunostaining images showing BrdU (red), DAPI (blue), and GAD67 (orange). Scale bars, 50 μm. **d**,**e**, The number of GAD67^{+} and/or BrdU^{+} cells in GL (**d**) and GCL (**e**). In **d** (GL; WT, n = 5; *Negr1*$^{-/-}$, n = 5), GAD67 and BrdU double positive cells (left; student's *t*-test, **P* = 0.421), GAD67 negative but BrdU positive cells (middle; student's t-test, *P* = 0.963), and total number of BrdU positive cells (right; student's t-test, **P* = 0.048). In **e** (GCL; WT, n = 5; *Negr1*$^{-/-}$, n = 5), GAD67 and BrdU double positive cells (left; student's *t*-test, *P* = 0.222), GAD67 negative but BrdU positive cells (middle; student's t-test, *P* = 0.243), and total number of BrdU positive cells (right; student's t-test, *P* = 0.605).

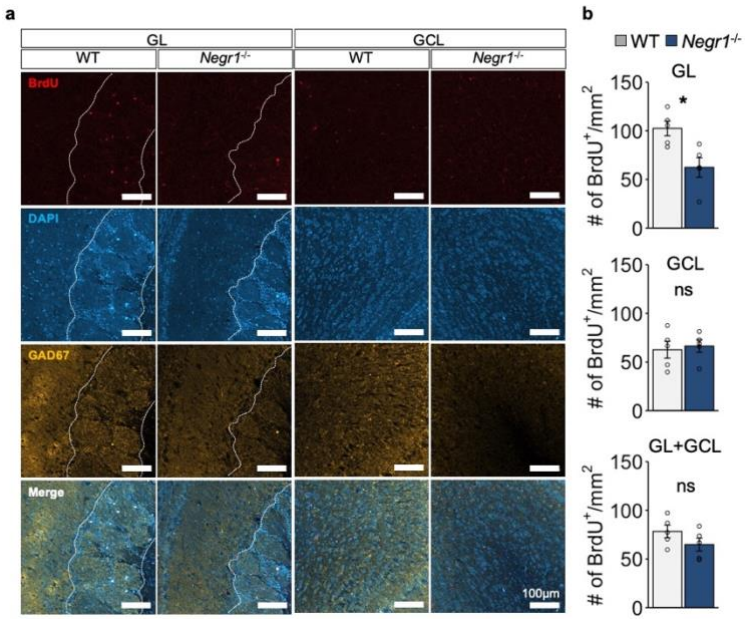

Figure 15. The number of newly generated cells is reduced in the GL of *Negr1*$^{-/-}$ mouse.

a, Immunostaining wide images of BrdU (red), DAPI (blue), and GAD67 (organge) in GL (left) and GCL (right). scale bars, 100 μm. **b**, The number of BrdU^{+} cells in GL (top; student's t-test, *P = 0.013), GCL (middle; student's t-test, P = 0.739), and both GL and GCL (bottom; student's t-test, P = 0.186).

3. CONCLUSION

3.1. Summary

Deficits in affective recognition is one of the key features of ASD patients (Fridenson-Hayo et al., 2016), but little is known about how mouse models of autism respond to the affective states of conspecifics. Here, I reveal that *Negr1* deficiency results in impairments in affective discrimination along with olfactory processing deficit. The co-manifestation of impairment in affective discrimination and olfactory processing in *Negr1*$^{-/-}$ mice allowed us to test whether neural alteration in the olfactory brain regions is involved in impaired affective recognition. I demonstrated that the excitability of olfactory mitral cells was decreased in *Negr1*$^{-/-}$ mice, with increased inhibitory synaptic transmissions. As a potential underlying mechanism, I found that adult olfactory neurogenesis was downregulated in the *Negr1*$^{-/-}$ mice, indicating that the defect in neuronal integration into the olfactory bulb may be responsible for the impaired olfactory processing and the affective discrimination in *Negr1*$^{-/-}$ mice (Figure 16)

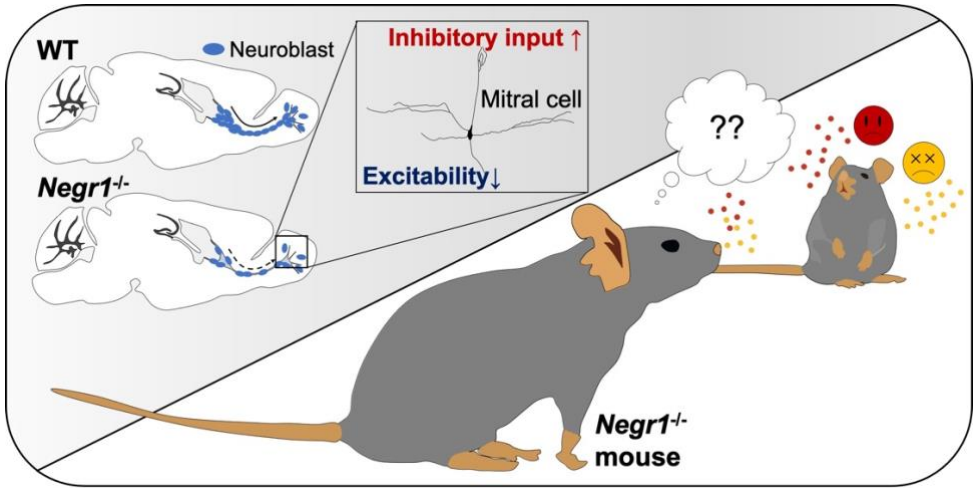

Figure 16. Graphical summary. *Negr1*-deficient mouse is impaired in discriminating affective states of other mice. The affective discrimination is associated with olfactory functions, in which the decrease in mitral cell excitability by *Negr1* deficiency can reduce efficiency of processing social olfactory information. The attenuated mitral cell excitability can be induced by increased inhibitory inputs, which can be related to the decrease in olfactory neurogenesis by *Negr1* deficiency.

3.2. Implication

In the present study, I demonstrated that *Negr1* deficiency impairs affective discrimination, resulting in unbiased social investigation regardless of the affective states of their conspecifics. This suggests that *Negr1* deficiency can disrupt the ability to recognize affective states in mice, which might induce inadequate motivational behaviors (i.e., approach or avoidance) to their conspecifics. In previous studies (Ferretti et al., 2019; Scheggia et al., 2020), normal mice showed preferential investigating behaviors depending on the affective states (e.g., stress, relief, fear) of conspecific, indicating affective information modulates motivation to interact with their conspecifics. However, as I observed in *Negr1*-deficient mice, the severity of ASD symptoms is negatively correlated with emotional reactivity and awareness, suggesting atypical emotional responses hindered engaging in social behaviors (Dijkhuis et al., 2019). According to the social motivation theory of autism, ASD people do not have an interest in others due to atypical processing of social stimuli regarding the generation of motivational valence in the brain circuit (Clements et al., 2018). However, the molecular entities underlying atypical information processing has remained elusive. The data in this study suggest that NEGR1 is involved in processing affective information to elicit social motivation. Of note, I found that *Negr1*$^{-/-}$ mice are impaired in habituation and dishabituation for social odors. This suggest that NEGR1 deficiency impairs social odor processing, which in turn disrupts the normal information transmission to the afferent pathway. Motivation-related brain areas, such as the basal nucleus of stria terminalis, cortical amygdala, and medial preoptic area, lie upstream of the olfactory pathway and are involved in social preference and consummatory social behaviors (Hu et al., 2021; Jones et al., 2011; Kim et al., 2015; Kwon et al., 2021). Thus, these findings suggest that *Negr1*-deficient mice aberrantly process social odors, which may prevent them from receiving intact social chemical signals in motivation-relevant brain areas. It is therefore conceivable that *Negr1*$^{-/-}$ mice are not motivated to interact with or avoid affective conspecifics because of impaired information processing of affective states of conspecifics.

In this study, I demonstrate that *Negr1*-deficient mice were distinct from WT mice in olfactory habituation, dishabituation, early affective discrimination, and

total affective discrimination. In addition, I found a positive correlation between social odor dishabituation and affective discrimination. This implies that the less dishabituated for changes in social odors mice are, the worse they are at discriminating conspecific affective states. Thus, *Negr1*-deficient mice are a useful mouse model to study the association between olfactory processing and affective recognition. Olfactory function and social-affective interaction are also associated with each other in people with ASD (Endevelt-Shapira et al., 2018; Rozenkrantz et al., 2015; Sweigert et al., 2020). For example, ASD children respond differently to (un)pleasant odors from typically-developed children, and this atypicality is associated with the social affect score of the autism diagnostic observation schedule (ADOS) (Rozenkrantz et al., 2015). Likewise, ASD children show abnormal autonomic response to fear-related body odor, which is also correlated with ADOS scores (Endevelt-Shapira et al., 2018). This indicates that autistic symptoms are linked with the olfactory function. Therefore, I suggest that *Negr1*-deficient mice are an appropriate animal model to dissect the underlying mechanism of ASD involving defects in olfactory sensory processing and affective recognition.

As for cellular mechanisms, I detected increased inhibitory synaptic inputs into and diminished excitability of olfactory mitral cells of *Negr1*-deficient mice. The increase in inhibitory inputs to the mitral cells can reduce their excitability, which in turn impair olfactory processing in *Negr1*-deficient mice. As the main output signaling for olfactory information, mitral cell temporal activity patterns are required to identify and discriminate odors accurately (Gschwend et al., 2012, 2015; Yamada et al., 2017). In this regard, inhibitory inputs to the mitral cell population may play roles in odor identification by tuning output properties (Cavarretta et al., 2016; Gschwend et al., 2015). Specifically, a subset of mitral cells, which fire spontaneously in the absence of any odor stimulation, is inhibited when an odor is presented (Kollo et al., 2014), and such temporal inhibition is critical for olfactory discrimination because it enhances signaling contrasts in response to odor stimuli (Wang et al., 2019). However, considering that mitral cell firing was suppressed at the basal level in *Negr1*$^{-/-}$ mice, olfactory signaling contrasts before and after odor presentation might be impaired, thereby resulting in the dysfunction of odor recognition.

Along with the functional alteration in the mitral cells, I showed that *Negr1* deficiency decreased neurogenesis in the adult olfactory bulb. The decreased olfactory neurogenesis in *Negr1*-deficient mice explains altered inhibitory inputs to the mitral cell population and the impaired olfactory processing of *Negr1*$^{-/-}$ mice. It has been reported that adult olfactory neurogenesis influences olfactory functions, such as odor discrimination and identification (Gheusi et al., 2000; Grelat et al., 2018; Moreno et al., 2009; Shani-Narkiss et al., 2020). Consistent with present findings, in particular, inhibiting adult-born olfactory neurons suppressed mitral cell activation and impaired odor discrimination (Shani-Narkiss et al., 2020). Adult-born interneurons have increased excitability with promiscuous connectivity within the olfactory microcircuit (Livneh et al., 2014), and this heightened basal excitability is maintained even after they are fully matured (Fomin-Thunemann et al., 2020). Considering olfactory interneurons inhibit other inhibitory neurons (i.e., lateral inhibition) and mitral cells, adult-born olfactory interneurons can transmit stronger and broader inhibitory outputs to both pre-existing inhibitory neurons and mitral cells. In a previous study, inhibiting adult-born interneurons reduced the dynamics of neuronal activity patterns in the microcircuit, and the basal and odor-evoked mitral cell activities were therefore unable to make contrast in electrical signals generated by olfactory stimuli (Shani-Narkiss et al., 2020). Thus, I hypothesized that the decrease in adult olfactory neurogenesis due to *Negr1* deficiency simultaneously reduces inhibitory outputs to pre-existing inhibitory neurons and mitral cells. Taken together, I argue that the impairment of olfactory information processing observed in *Negr1*-deficient mice is at least partly due to the decrease in adult olfactory neurogenesis with an inefficient signal transmission within the OB.

3.3. Limitation and Future Research

In this study, there are some limitations that will be addressed in future work. First, I did not identify mechanisms to explain how NEGR1 deficiency affects olfactory neurogenesis. In a previous study, NEGR1 modulates adult hippocampal neurogenesis by interacting with the leukemia inhibitory factor (LIF) receptor and inducing lipocalin-2 expression (Noh et al., 2019). LIF receptor in SVZ, however, has been reported to downregulate neurogenesis in the presence of LIF (Bauer &

Patterson, 2006). Thus, it is not likely that NEGR1 contributes to olfactory neurogenesis by interacting with the LIF receptor. Instead, NEGR1 forms a heterodimer with fibroblast growth factor receptor 2 (FGFR2), which supports the downstream signaling of FGFR2 (Szczurkowska et al., 2018). The FGFR2 is known to be expressed and promotes adult neurogenesis within SVZ (Chadashvili & Peterson, 2006; Frinchi et al., 2008). Therefore, it is conceivable that NEGR1 plays a role in adult olfactory neurogenesis by interacting with FGFR2, a relationship that needs to be tested in the future studies by identifying the expression level of FGFR2 with western blot and qPCR, then comparing the amount of neurogenic marker proteins between WT and *Neg1*-deficient mouse after overexpressing FGFR2 level in the SVZ.

Second, I did not clearly address the difference in olfactory behavioral reactivity between the novel (water, banana, and almond) and familiar (a regular chow) non-social odors in *Negr1*-deficient mice. According to a previous study (Magavi et al., 2005), adult-born olfactory neurons are involved in an initial response to a novel odor and odor familiarization. When assessing the response of *c-fos*, one of the immediate early genes, in the OB, the expression level of *c-fos* was increased in adult-born neurons after mice were exposed to the odor not only for the first time (i.e., novel condition) but after consecutive three days (i.e., familiarization condition) compared to preexisting neurons. This may explain the insensitive reaction to novel odors and the failure to associate a reward with novel odors during the four-day learning phase in the *Negr1*-deficient mouse. To confirm the involvement of adult-born neurons in the behavioral aberrations in *Negr1*-deficient mice, *in vivo* calcium recordings for OB neurons can be employed to observe neuronal signaling dynamics at an initial response to novel odors as well as during and after associating a reward with odors.

3.4. Concluding Remarks

Conclusively, I showed that *Negr1* deficiency, a risk factor gene of ASD, leads to deficits in social-affective discrimination and abnormal olfactory processing with reduced OB neurogenesis. These data reveal an unexpected link between affective recognition and olfactory processing mediated by NEGR1, and I propose a novel neurobiological mechanism of autism-related behaviors based on disrupted adult olfactory neurogenesis and processing.

BIBLIOGRAPHY

Bariselli, S., Tzanoulinou, S., Glangetas, C., Prévost-Solié, C., Pucci, L., Viguié, J., Bezzi, P., O'Connor, E. C., Georges, F., Lüscher, C., & Bellone, C. (2016). SHANK3 controls maturation of social reward circuits in the VTA. *Nature Neuroscience*, *19*(7), Article 7. doi:10.1038/nn.4319

Bartal, I. B.-A., Decety, J., & Mason, P. (2011). Empathy and Pro-Social Behavior in Rats. *Science*, *334*(6061), 1427–1430. doi:10.1126/science.1210789

Bauer, S., & Patterson, P. H. (2006). Leukemia Inhibitory Factor Promotes Neural Stem Cell Self-Renewal in the Adult Brain. *Journal of Neuroscience*, *26*(46), 12089–12099. doi:10.1523/JNEUROSCI.3047-06.2006

Benson, V., Castelhano, M. S., Howard, P. L., Latif, N., & Rayner, K. (2016). Looking, seeing and believing in autism: Eye movements reveal how subtle cognitive processing differences impact in the social domain. *Autism Research*, *9*(8), 879–887. doi:10.1002/aur.1580

Birey, F., Li, M.-Y., Gordon, A., Thete, M. V., Valencia, A. M., Revah, O., Paşca, A. M., Geschwind, D. H., & Paşca, S. P. (2022). Dissecting the molecular basis of human interneuron migration in forebrain assembloids from Timothy syndrome. *Cell Stem Cell*, *29*(2), 248-264.e7. doi:10.1016/j.stem.2021.11.011

Cavarretta, F., Marasco, A., Hines, M. L., Shepherd, G. M., & Migliore, M. (2016). Glomerular and Mitral-Granule Cell Microcircuits Coordinate Temporal and Spatial Information Processing in the Olfactory Bulb. *Frontiers in Computational Neuroscience*, *10*. doi:10.3389/fncom.2016.00067

Chadashvili, T., & Peterson, D. A. (2006). Cytoarchitecture of fibroblast growth factor receptor 2 (FGFR-2) immunoreactivity in astrocytes of neurogenic and non-neurogenic regions of the young adult and aged rat brain. *Journal of Comparative Neurology*, *498*(1), 1–15. doi:10.1002/cne.21009

Chaplan, S. R., Bach, F. W., Pogrel, J. W., Chung, J. M., & Yaksh, T. L. (1994). Quantitative assessment of tactile allodynia in the rat paw. *Journal of Neuroscience Methods*, *53*(1), 55–63. doi:10.1016/0165-0270(94)90144-9

Chazal, G., Durbec, P., Jankovski, A., Rougon, G., & Cremer, H. (2000). Consequences of Neural Cell Adhesion Molecule Deficiency on Cell Migration in

the Rostral Migratory Stream of the Mouse. *Journal of Neuroscience*, *20*(4), 1446–1457. doi:10.1523/JNEUROSCI.20-04-01446.2000

Clements, C. C., Zoltowski, A. R., Yankowitz, L. D., Yerys, B. E., Schultz, R. T., & Herrington, J. D. (2018). Evaluation of the Social Motivation Hypothesis of Autism: A Systematic Review and Meta-analysis. *JAMA Psychiatry*, *75*(8), 797–808. doi:10.1001/jamapsychiatry.2018.1100

Contestabile, A., Casarotto, G., Girard, B., Tzanoulinou, S., & Bellone, C. (2021). Deconstructing the contribution of sensory cues in social approach. *European Journal of Neuroscience*, *53*(9), 3199–3211. doi:10.1111/ejn.15179

Curtis, M. A., Kam, M., Nannmark, U., Anderson, M. F., Axell, M. Z., Wikkelso, C., Holtås, S., van Roon-Mom, W. M. C., Björk-Eriksson, T., Nordborg, C., Frisén, J., Dragunow, M., Faull, R. L. M., & Eriksson, P. S. (2007). Human Neuroblasts Migrate to the Olfactory Bulb via a Lateral Ventricular Extension. *Science*, *315*(5816), 1243–1249. doi:10.1126/science.1136281

Dalton, K. M., Nacewicz, B. M., Johnstone, T., Schaefer, H. S., Gernsbacher, M. A., Goldsmith, H. H., Alexander, A. L., & Davidson, R. J. (2005). Gaze fixation and the neural circuitry of face processing in autism. *Nature Neuroscience*, *8*(4), Article 4. doi:10.1038/nn1421

Davies, M. S., Dapretto, M., Sigman, M., Sepeta, L., & Bookheimer, S. Y. (2011). Neural bases of gaze and emotion processing in children with autism spectrum disorders. *Brain and Behavior*, *1*(1), 1–11. doi:10.1002/brb3.6

Deeley, Q., Daly, E. M., Surguladze, S., Page, L., Toal, F., Robertson, D., Curran, S., Giampietro, V., Seal, M., Brammer, M. J., Andrew, C., Murphy, K., Phillips, M. L., & Murphy, D. G. M. (2007). An Event Related Functional Magnetic Resonance Imaging Study of Facial Emotion Processing in Asperger Syndrome. *Biological Psychiatry*, *62*(3), 207–217. doi:10.1016/j.biopsych.2006.09.037

Dijkhuis, R., Gurbuz, E., Ziermans, T., Staal, W., & Swaab, H. (2019). Social Attention and Emotional Responsiveness in Young Adults With Autism. *Frontiers in Psychiatry*, *10*. doi:10.3389/fpsyt.2019.00426

Doetsch, F., & Alvarez-Buylla, A. (1996). Network of tangential pathways for neuronal migration in adult mammalian brain. *Proceedings of the National Academy of Sciences*, *93*(25), 14895–14900. doi:10.1073/pnas.93.25.14895

Dolensek, N., Gehrlach, D. A., Klein, A. S., & Gogolla, N. (2020). Facial expressions of emotion states and their neuronal correlates in mice. *Science*, *368*(6486), 89–94. doi:10.1126/science.aaz9468

Doucette, W., Gire, D. H., Whitesell, J., Carmean, V., Lucero, M. T., & Restrepo, D. (2011). Associative Cortex Features in the First Olfactory Brain Relay Station. *Neuron*, *69*(6), 1176–1187. doi:10.1016/j.neuron.2011.02.024

Endevelt-Shapira, Y., Perl, O., Ravia, A., Amir, D., Eisen, A., Bezalel, V., Rozenkrantz, L., Mishor, E., Pinchover, L., Soroka, T., Honigstein, D., & Sobel, N. (2018). Altered responses to social chemosignals in autism spectrum disorder. *Nature Neuroscience*, *21*(1), Article 1. doi:10.1038/s41593-017-0024-x

Feierstein, C., Lazarini, F., Wagner, S., Gabellec, M.-M., De Chaumont, F., Olivo-Marin, J.-C., Boussin, F., Lledo, P., & Gheusi, G. (2010). Disruption of Adult Neurogenesis in the Olfactory Bulb Affects Social Interaction but not Maternal Behavior. *Frontiers in Behavioral Neuroscience*, *4*. doi:10.3389/fnbeh.2010.00176

Ferretti, V., Maltese, F., Contarini, G., Nigro, M., Bonavia, A., Huang, H., Gigliucci, V., Morelli, G., Scheggia, D., Managò, F., Castellani, G., Lefevre, A., Cancedda, L., Chini, B., Grinevich, V., & Papaleo, F. (2019). Oxytocin Signaling in the Central Amygdala Modulates Emotion Discrimination in Mice. *Current Biology*, *29*(12), 1938-1953.e6. doi:10.1016/j.cub.2019.04.070

Fomin-Thunemann, N., Kovalchuk, Y., Fink, S., Alsema, A., Mojtahedi, N., Zirdum, E., & Garaschuk, O. (2020). Unique Functional Properties of Mature Adult-Born Neurons in the Mouse Olfactory Bulb. *Stem Cell Reports*, *15*(6), 1333–1346. doi:10.1016/j.stemcr.2020.10.010

Fridenson-Hayo, S., Berggren, S., Lassalle, A., Tal, S., Pigat, D., Bölte, S., Baron-Cohen, S., & Golan, O. (2016). Basic and complex emotion recognition in children with autism: Cross-cultural findings. *Molecular Autism*, *7*(1), 52. doi:10.1186/s13229-016-0113-9

Frinchi, M., Bonomo, A., Trovato-Salinaro, A., Condorelli, D. F., Fuxe, K., Spampinato, M. G., & Mudò, G. (2008). Fibroblast growth factor-2 and its receptor expression in proliferating precursor cells of the subventricular zone in the adult rat brain. *Neuroscience Letters*, *447*(1), 20–25. doi:10.1016/j.neulet.2008.09.059

Funatsu, N., Miyata, S., Kumanogoh, H., Shigeta, M., Hamada, K., Endo, Y., Sokawa, Y., & Maekawa, S. (1999). Characterization of a Novel Rat Brain

Glycosylphosphatidylinositol-anchored Protein (Kilon), a Member of the IgLON Cell Adhesion Molecule Family*. *Journal of Biological Chemistry*, *274*(12), 8224–8230. doi:10.1074/jbc.274.12.8224

Galle, S. A., Courchesne, V., Mottron, L., & Frasnelli, J. (2013). Olfaction in the Autism Spectrum. *Perception*, *42*(3), 341–355. doi:10.1068/p7337

Gheusi, G., Cremer, H., McLean, H., Chazal, G., Vincent, J.-D., & Lledo, P.-M. (2000). Importance of newly generated neurons in the adult olfactory bulb for odor discrimination. *Proceedings of the National Academy of Sciences*, *97*(4), 1823–1828. doi:10.1073/pnas.97.4.1823

Gire, D. H., Whitesell, J. D., Doucette, W., & Restrepo, D. (2013). Information for decision-making and stimulus identification is multiplexed in sensory cortex. *Nature Neuroscience*, *16*(8), Article 8. doi:10.1038/nn.3432

Grelat, A., Benoit, L., Wagner, S., Moigneu, C., Lledo, P.-M., & Alonso, M. (2018). Adult-born neurons boost odor–reward association. *Proceedings of the National Academy of Sciences*, *115*(10), 2514–2519. doi:10.1073/pnas.1716400115

Grove, J., Ripke, S., Als, T. D., Mattheisen, M., Walters, R. K., Won, H., Pallesen, J., Agerbo, E., Andreassen, O. A., Anney, R., Awashti, S., Belliveau, R., Bettella, F., Buxbaum, J. D., Bybjerg-Grauholm, J., Bækvad-Hansen, M., Cerrato, F., Chambert, K., Christensen, J. H., … Børglum, A. D. (2019). Identification of common genetic risk variants for autism spectrum disorder. *Nature Genetics*, *51*(3), Article 3. doi:10.1038/s41588-019-0344-8

Gschwend, O., Abraham, N. M., Lagier, S., Begnaud, F., Rodriguez, I., & Carleton, A. (2015). Neuronal pattern separation in the olfactory bulb improves odor discrimination learning. *Nature Neuroscience*, *18*(10), Article 10. doi:10.1038/nn.4089

Gschwend, O., Beroud, J., & Carleton, A. (2012). Encoding Odorant Identity by Spiking Packets of Rate-Invariant Neurons in Awake Mice. *PLOS ONE*, *7*(1), e30155. doi:10.1371/journal.pone.0030155

Guarnieri, L. O., Pereira-Caixeta, A. R., Medeiros, D. C., Aquino, N. S. S., Szawka, R. E., Mendes, E. M. A. M., Moraes, M. F. D., & Pereira, G. S. (2020). Pro-neurogenic effect of fluoxetine in the olfactory bulb is concomitant to improvements in social memory and depressive-like behavior of socially isolated mice. *Translational Psychiatry*, *10*(1), Article 1. doi:10.1038/s41398-020-0701-5

Hashimoto, T., Maekawa, S., & Miyata, S. (2009). IgLON cell adhesion molecules regulate synaptogenesis in hippocampal neurons. *Cell Biochemistry and Function*, *27*(7), 496–498. doi:10.1002/cbf.1600

Hedley, D., Young, R., & Brewer, N. (2012). Using Eye Movements as an Index of Implicit Face Recognition in Autism Spectrum Disorder. *Autism Research*, *5*(5), 363–379. doi:10.1002/aur.1246

Hornberg, H., Pérez-Garci, E., Schreiner, D., Hatstatt-Burklé, L., Magara, F., Baudouin, S., Matter, A., Nacro, K., Pecho-Vrieseling, E., & Scheiffele, P. (2020). Rescue of oxytocin response and social behaviour in a mouse model of autism. *Nature*, *584*(7820), Article 7820. doi:10.1038/s41586-020-2563-7

Hu, R. K., Zuo, Y., Ly, T., Wang, J., Meera, P., Wu, Y. E., & Hong, W. (2021). An amygdala-to-hypothalamus circuit for social reward. *Nature Neuroscience*, *24*(6), Article 6. doi:10.1038/s41593-021-00828-2

Imayoshi, I., Sakamoto, M., Ohtsuka, T., Takao, K., Miyakawa, T., Yamaguchi, M., Mori, K., Ikeda, T., Itohara, S., & Kageyama, R. (2008). Roles of continuous neurogenesis in the structural and functional integrity of the adult forebrain. *Nature Neuroscience*, *11*(10), Article 10. doi:10.1038/nn.2185

Jagomae, T., Singh, K., Philips, M.-A., Jayaram, M., Seppa, K., Tekko, T., Gilbert, S. F., Vasar, E., & Lilleväli, K. (2021). Alternative Promoter Use Governs the Expression of IgLON Cell Adhesion Molecules in Histogenetic Fields of the Embryonic Mouse Brain. *International Journal of Molecular Sciences*, *22*(13), Article 13. doi:10.3390/ijms22136955

Jeon, D., Kim, S., Chetana, M., Jo, D., Ruley, H. E., Lin, S.-Y., Rabah, D., Kinet, J.-P., & Shin, H.-S. (2010). Observational fear learning involves affective pain system and Cav1.2 Ca2+ channels in ACC. *Nature Neuroscience*, *13*(4), Article 4. doi:10.1038/nn.2504

Jones, R. M., Somerville, L. H., Li, J., Ruberry, E. J., Libby, V., Glover, G., Voss, H. U., Ballon, D. J., & Casey, B. J. (2011). Behavioral and Neural Properties of Social Reinforcement Learning. *Journal of Neuroscience*, *31*(37), 13039–13045. doi:10.1523/JNEUROSCI.2972-11.2011

Kim, H., Cho, B., Park, H., Kim, J., Kim, S., Shin, J., Lengner, C. J., Won, K.-J., & Kim, J. (2022). Dormant state of quiescent neural stem cells links Shank3

mutation to autism development. *Molecular Psychiatry*, *27*(6), Article 6. doi:10.1038/s41380-022-01563-1

Kim, Y., Venkataraju, K. U., Pradhan, K., Mende, C., Taranda, J., Turaga, S. C., Arganda-Carreras, I., Ng, L., Hawrylycz, M. J., Rockland, K. S., Seung, H. S., & Osten, P. (2015). Mapping Social Behavior-Induced Brain Activation at Cellular Resolution in the Mouse. *Cell Reports*, *10*(2), 292–305. doi:10.1016/j.celrep.2014.12.014

Kleinhans, N. M., Richards, T., Johnson, L. C., Weaver, K. E., Greenson, J., Dawson, G., & Aylward, E. (2011). FMRI evidence of neural abnormalities in the subcortical face processing system in ASD. *NeuroImage*, *54*(1), 697–704. doi10.1016/j.neuroimage.2010.07.037

Kollo, M., Schmaltz, A., Abdelhamid, M., Fukunaga, I., & Schaefer, A. T. (2014). "Silent" mitral cells dominate odor responses in the olfactory bulb of awake mice. *Nature Neuroscience*, *17*(10), Article 10. doi:10.1038/nn.3768

Kornack, D. R., & Rakic, P. (2001). The generation, migration, and differentiation of olfactory neurons in the adult primate brain. *Proceedings of the National Academy of Sciences*, *98*(8), 4752–4757. doi:10.1073/pnas.081074998

Kovalchuk, Y., Homma, R., Liang, Y., Maslyukov, A., Hermes, M., Thestrup, T., Griesbeck, O., Ninkovic, J., Cohen, L. B., & Garaschuk, O. (2015). In vivo odourant response properties of migrating adult-born neurons in the mouse olfactory bulb. *Nature Communications*, *6*(1), Article 1. doi:10.1038/ncomms7349

Kristensen, H. H., Jones, R. B., Schofield, C. P., White, R. P., & Wathes, C. M. (2001). The use of olfactory and other cues for social recognition by juvenile pigs. *Applied Animal Behaviour Science*, *72*(4), 321–333. doi:10.1016/S0168-1591(00)00209-4

Kwak, J.-H., Lee, Y., Jun, M.-H., Roh, M., Seo, H., Lee, J., Lee, K., & Lee, J.-A. (2021). Autophagy activity contributes to the impairment of social recognition in Epac2−/− mice. *Molecular Brain*, *14*(1), 100. doi:10.1186/s13041-021-00814-6

Kwon, J.-T., Ryu, C., Lee, H., Sheffield, A., Fan, J., Cho, D. H., Bigler, S., Sullivan, H. A., Choe, H. K., Wickersham, I. R., Heiman, M., & Choi, G. B. (2021). An amygdala circuit that suppresses social engagement. *Nature*, *593*(7857), Article 7857. doi:10.1038/s41586-021-03413-6

Langford, D. J., Bailey, A. L., Chanda, M. L., Clarke, S. E., Drummond, T. E., Echols, S., Glick, S., Ingrao, J., Klassen-Ross, T., LaCroix-Fralish, M. L.,

Matsumiya, L., Sorge, R. E., Sotocinal, S. G., Tabaka, J. M., Wong, D., van den Maagdenberg, A. M. J. M., Ferrari, M. D., Craig, K. D., & Mogil, J. S. (2010). Coding of facial expressions of pain in the laboratory mouse. *Nature Methods*, *7*(6), Article 6. doi:10.1038/nmeth.1455

Levy, D. R., Tamir, T., Kaufman, M., Parabucki, A., Weissbrod, A., Schneidman, E., & Yizhar, O. (2019). Dynamics of social representation in the mouse prefrontal cortex. *Nature Neuroscience*, *22*(12), Article 12. doi:10.1038/s41593-019-0531-z

Li, Y., Luo, Z.-Y., Hu, Y.-Y., Bi, Y.-W., Yang, J.-M., Zou, W.-J., Song, Y.-L., Li, S., Shen, T., Li, S.-J., Huang, L., Zhou, A.-J., Gao, T.-M., & Li, J.-M. (2020). The gut microbiota regulates autism-like behavior by mediating vitamin B6 homeostasis in EphB6-deficient mice. *Microbiome*, *8*(1), 120. doi:10.1186/s40168-020-00884-z

Lim, C.-S., Kim, M. J., Choi, J. E., Islam, M. A., Lee, Y.-K., Xiong, Y., Shim, K.-W., Yang, J., Lee, R. U., Lee, J., Park, P., Kwak, J.-H., Seo, H., Kim, C. H., Lee, J.-H., Lee, Y.-S., Hwang, S.-K., Lee, K., Lee, J.-A., & Kaang, B.-K. (2021). Dysfunction of NMDA receptors in neuronal models of an autism spectrum disorder patient with a DSCAM mutation and in Dscam-knockout mice. *Molecular Psychiatry*, *26*(12), Article 12. doi:10.1038/s41380-021-01216-9

Lim, H., Lee, H., Noh, K., & Lee, S. J. (2017). IKK/NF-κB-dependent satellite glia activation induces spinal cord microglia activation and neuropathic pain after nerve injury. *PAIN*, *158*(9), 1666–1677. doi:10.1097/j.pain.0000000000000959

Lim, S.-H., Kwon, S.-K., Lee, M. K., Moon, J., Jeong, D. G., Park, E., Kim, S. J., Park, B. C., Lee, S. C., Ryu, S.-E., Yu, D.-Y., Chung, B. H., Kim, E., Myung, P.-K., & Lee, J.-R. (2009). Synapse formation regulated by protein tyrosine phosphatase receptor T through interaction with cell adhesion molecules and Fyn. *The EMBO Journal*, *28*(22), 3564–3578. doi:10.1038/emboj.2009.289

Liu, Z., Chen, Z., Shang, C., Yan, F., Shi, Y., Zhang, J., Qu, B., Han, H., Wang, Y., Li, D., Südhof, T. C., & Cao, P. (2017). IGF1-Dependent Synaptic Plasticity of Mitral Cells in Olfactory Memory during Social Learning. *Neuron*, *95*(1), 106-122.e5. doi:10.1016/j.neuron.2017.06.015

Livneh, Y., Adam, Y., & Mizrahi, A. (2014). Odor Processing by Adult-Born Neurons. *Neuron*, *81*(5), 1097–1110. doi:10.1016/j.neuron.2014.01.007

Lois, C. & Alvarez-Buylla, A. (1994). Long-Distance Neuronal Migration in the Adult Mammalian Brain. *Science*, *264*(5162), 1145–1148. doi:10.1126/science.8178174

Magavi, S. S. P., Mitchell, B. D., Szentirmai, O., Carter, B. S., and Macklis, J. D. (2005). Adult-born and preexisiting olfactory granule neurons undergo distinct experience-dependent modifications of their olfactory responses in vivo. Journal of Neuroscience, 25(46), 10729–10739. doi:10.1523/JNEUROSCI.2250-05.2005

Mateo, J. M. (2009). The causal role of odours in the development of recognition templates and social preferences. *Animal Behaviour*, *77*(1), 115–121. doi:10.1016/j.anbehav.2008.09.015

Merkle, F. T., Fuentealba, L. C., Sanders, T. A., Magno, L., Kessaris, N., & Alvarez-Buylla, A. (2014). Adult neural stem cells in distinct microdomains generate previously unknown interneuron types. *Nature Neuroscience*, *17*(2), Article 2. doi:10.1038/nn.3610

Merkle, F. T., Mirzadeh, Z., & Alvarez-Buylla, A. (2007). Mosaic Organization of Neural Stem Cells in the Adult Brain. *Science*, *317*(5836), 381–384. doi:10.1126/science.1144914

Mishor, E., Amir, D., Weiss, T., Honigstein, D., Weissbrod, A., Livne, E., Gorodisky, L., Karagach, S., Ravia, A., Snitz, K., Karawani, D., Zirler, R., Weissgross, R., Soroka, T., Endevelt-Shapira, Y., Agron, S., Rozenkrantz, L., Reshef, N., Furman-Haran, E., … Sobel, N. (2021). Sniffing the human body volatile hexadecanal blocks aggression in men but triggers aggression in women. *Science Advances*, *7*(47), eabg1530. doi:10.1126/sciadv.abg1530

Miyata, S., Taguchi, K., & Maekawa, S. (2003). Dendrite-associated opioid-binding cell adhesion molecule localizes at neurosecretory granules in the hypothalamic magnocellular neurons. *Neuroscience*, *122*(1), 169–181. doi:10.1016/S0306-4522(03)00609-2

Moore, A., Chinnaiya, K., Kim, D. W., Brown, S., Stewart, I., Robins, S., Dowsett, G. K. C., Muir, C., Travaglio, M., Lewis, J. E., Ebling, F., Blackshaw, S., Furley, A., & Placzek, M. (2022). Loss of Function of the Neural Cell Adhesion Molecule NrCAM Regulates Differentiation, Proliferation and Neurogenesis in Early Postnatal Hypothalamic Tanycytes. *Frontiers in Neuroscience*, *16*. doi:10.3389/fnins.2022.832961

Moreno, M. M., Linster, C., Escanilla, O., Sacquet, J., Didier, A., & Mandairon, N. (2009). Olfactory perceptual learning requires adult neurogenesis. *Proceedings of the National Academy of Sciences*, *106*(42), 17980–17985. doi:10.1073/pnas.0907063106

Mujica-Parodi, L. R., Strey, H. H., Frederick, B., Savoy, R., Cox, D., Botanov, Y., Tolkunov, D., Rubin, D., & Weber, J. (2009). Chemosensory Cues to Conspecific Emotional Stress Activate Amygdala in Humans. *PLOS ONE*, *4*(7), e6415. doi:10.1371/journal.pone.0006415

Nakamura, M., Ye, K., e Silva, M. B., Yamauchi, T., Hoeppner, D. J., Fayyazuddin, A., Kang, G., Yuda, E. A., Nagashima, M., Enomoto, S., Hiramoto, T., Sharp, R., Kaneko, I., Tajinda, K., Adachi, M., Mihara, T., Tokuno, S., Geyer, M. A., Broin, P. Ó., … Hiroi, N. (2021). Computational identification of variables in neonatal vocalizations predictive for postpubertal social behaviors in a mouse model of 16p11.2 deletion. *Molecular Psychiatry*, *26*(11), Article 11. doi:10.1038/s41380-021-01089-y

Noh, K., Lee, H., Choi, T.-Y., Joo, Y., Kim, S.-J., Kim, H., Kim, J. Y., Jahng, J. W., Lee, S., Choi, S.-Y., & Lee, S. J. (2019). Negr1 controls adult hippocampal neurogenesis and affective behaviors. *Molecular Psychiatry*, *24*(8), Article 8. doi:10.1038/s41380-018-0347-3

Oettl, L.-L., Ravi, N., Schneider, M., Scheller, M. F., Schneider, P., Mitre, M., da Silva Gouveia, M., Froemke, R. C., Chao, M. V., Young, W. S., Meyer-Lindenberg, A., Grinevich, V., Shusterman, R., & Kelsch, W. (2016). Oxytocin Enhances Social Recognition by Modulating Cortical Control of Early Olfactory Processing. *Neuron*, *90*(3), 609–621. doi:10.1016/j.neuron.2016.03.033

Penagarikano, O., Abrahams, B. S., Herman, E. I., Winden, K. D., Gdalyahu, A., Dong, H., Sonnenblick, L. I., Gruver, R., Almajano, J., Bragin, A., Golshani, P., Trachtenberg, J. T., Peles, E., & Geschwind, D. H. (2011). Absence of CNTNAP2 Leads to Epilepsy, Neuronal Migration Abnormalities, and Core Autism-Related Deficits. *Cell*, *147*(1), 235–246. doi:10.1016/j.cell.2011.08.040

Penagarikano, O., Lázaro, M. T., Lu, X.-H., Gordon, A., Dong, H., Lam, H. A., Peles, E., Maidment, N. T., Murphy, N. P., Yang, X. W., Golshani, P., & Geschwind, D. H. (2015). Exogenous and evoked oxytocin restores social

behavior in the Cntnap2 mouse model of autism. *Science Translational Medicine*, *7*(271), 271ra8-271ra8. doi:10.1126/scitranslmed.3010257

Pesa, J., Feliciano, C., Ting, J. T., Wang, W., Wells, M. F., Venkatraman, T. N., Lascola, C. D., Fu, Z., & Feng, G. (2011). Shank3 mutant mice display autistic-like behaviours and striatal dysfunction. *Nature*, *472*(7344), Article 7344. doi:10.1038/nature09965

Pischedda, F., & Piccoli, G. (2016). The IgLON Family Member Negr1 Promotes Neuronal Arborization Acting as Soluble Factor via FGFR2. *Frontiers in Molecular Neuroscience*, *0*. doi:10.3389/fnmol.2015.00089

Pool, E., Delplanque, S., Porcherot, C., Jenkins, T., Cayeux, I., & Sander, D. (2014). Sweet reward increases implicit discrimination of similar odors. *Frontiers in Behavioral Neuroscience*, *8*. doi:10.3389/fnbeh.2014.00158

Ravreby, I., Snitz, K., & Sobel, N. (2022). There is chemistry in social chemistry. *Science Advances*, *8*(25), eabn0154. doi:10.1126/sciadv.abn0154

Reed, M. D., Yim, Y. S., Wimmer, R. D., Kim, H., Ryu, C., Welch, G. M., Andina, M., King, H. O., Waisman, A., Halassa, M. M., Huh, J. R., & Choi, G. B. (2020). IL-17a promotes sociability in mouse models of neurodevelopmental disorders. *Nature*, *577*(7789), Article 7789. doi:10.1038/s41586-019-1843-6

Rogers-Carter, M. M., Varela, J. A., Gribbons, K. B., Pierce, A. F., McGoey, M. T., Ritchey, M., & Christianson, J. P. (2018). Insular cortex mediates approach and avoidance responses to social affective stimuli. *Nature Neuroscience*, *21*(3), Article 3. doi:10.1038/s41593-018-0071-y

Rozenkrantz, L., Zachor, D., Heller, I., Plotkin, A., Weissbrod, A., Snitz, K., Secundo, L., & Sobel, N. (2015). A Mechanistic Link between Olfaction and Autism Spectrum Disorder. *Current Biology*, *25*(14), 1904–1910. doi:10.1016/j.cub.2015.05.048

Sakamoto, M., Imayoshi, I., Ohtsuka, T., Yamaguchi, M., Mori, K., & Kageyama, R. (2011). Continuous neurogenesis in the adult forebrain is required for innate olfactory responses. *Proceedings of the National Academy of Sciences*, *108*(20), 8479–8484. doi:10.1073/pnas.1018782108

Sanai, N., Nguyen, T., Ihrie, R. A., Mirzadeh, Z., Tsai, H.-H., Wong, M., Gupta, N., Berger, M. S., Huang, E., Garcia-Verdugo, J.-M., Rowitch, D. H., & Alvarez-Buylla, A. (2011). Corridors of migrating neurons in the human brain

and their decline during infancy. *Nature*, *478*(7369), Article 7369. doi:10.1038/nature10487

Sanders, A. F. P., Hobbs, D. A., Knaus, T. A., & Beaton, E. A. (2022). Structural Connectivity and Emotion Recognition Impairment in Children and Adolescents with Chromosome 22q11.2 Deletion Syndrome. *Journal of Autism and Developmental Disorders*. doi:10.1007/s10803-022-05675-z

Sanz, R., Ferraro, G. B., & Fournier, A. E. (2015). IgLON Cell Adhesion Molecules Are Shed from the Cell Surface of Cortical Neurons to Promote Neuronal Growth*. *Journal of Biological Chemistry*, *290*(7), 4330–4342. doi:10.1074/jbc.M114.628438

Scheggia, D., Managò, F., Maltese, F., Bruni, S., Nigro, M., Dautan, D., Latuske, P., Contarini, G., Gomez-Gonzalo, M., Requie, L. M., Ferretti, V., Castellani, G., Mauro, D., Bonavia, A., Carmignoto, G., Yizhar, O., & Papaleo, F. (2020). Somatostatin interneurons in the prefrontal cortex control affective state discrimination in mice. *Nature Neuroscience*, *23*(1), Article 1. doi:10.1038/s41593-019-0551-8

Shani-Narkiss, H., Vinograd, A., Landau, I. D., Tasaka, G., Yayon, N., Terletsky, S., Groysman, M., Maor, I., Sompolinsky, H., & Mizrahi, A. (2020). Young adult-born neurons improve odor coding by mitral cells. *Nature Communications*, *11*(1), Article 1. doi:10.1038/s41467-020-19472-8

Singh, K., Lilleväli, K., Gilbert, S. F., Bregin, A., Narvik, J., Jayaram, M., Rahi, M., Innos, J., Kaasik, A., Vasar, E., & Philips, M.-A. (2018a). The combined impact of IgLON family proteins Lsamp and Neurotrimin on developing neurons and behavioral profiles in mouse. *Brain Research Bulletin*, *140*, 5–18. doi:10.1016/j.brainresbull.2018.03.013

Singh, K., Loreth, D., Pöttker, B., Hefti, K., Innos, J., Schwald, K., Hengstler, H., Menzel, L., Sommer, C. J., Radyushkin, K., Kretz, O., Philips, M.-A., Haas, C. A., Frauenknecht, K., Lilleväli, K., Heimrich, B., Vasar, E., & Schäfer, M. K. E. (2018b). Neuronal Growth and Behavioral Alterations in Mice Deficient for the Psychiatric Disease-Associated Negr1 Gene. *Frontiers in Molecular Neuroscience*, *11*. doi:10.3389/fnmol.2018.00030

Smith, M. L., Asada, N., & Malenka, R. C. (2021). Anterior cingulate inputs to nucleus accumbens control the social transfer of pain and analgesia. *Science*, *371*(6525), 153–159. doi:10.1126/science.abe3040

Sweigert, J. R., St. John, T., Begay, K. K., Davis, G. E., Munson, J., Shankland, E., Estes, A., Dager, S. R., & Kleinhans, N. M. (2020). Characterizing Olfactory Function in Children with Autism Spectrum Disorder and Children with Sensory Processing Dysfunction. *Brain Sciences*, *10*(6), Article 6. doi:10.3390/brainsci10060362

Szczurkowska, J., Pischedda, F., Pinto, B., Managò, F., Haas, C. A., Summa, M., Bertorelli, R., Papaleo, F., Schäfer, M. K., Piccoli, G., & Cancedda, L. (2018). NEGR1 and FGFR2 cooperatively regulate cortical development and core behaviours related to autism disorders in mice. *Brain*, *141*(9), 2772–2794. doi:10.1093/brain/awy190

Takahashi, H., Ogawa, Y., Yoshihara, S., Asahina, R., Kinoshita, M., Kitano, T., Kitsuki, M., Tatsumi, K., Okuda, M., Tatsumi, K., Wanaka, A., Hirai, H., Stern, P. L., & Tsuboi, A. (2016). A Subtype of Olfactory Bulb Interneurons Is Required for Odor Detection and Discrimination Behaviors. *Journal of Neuroscience*, *36*(31), 8210–8227. doi:10.1523/JNEUROSCI.2783-15.2016

Valley, M., Mullen, T., Schultz, L., Sagdullaev, B., & Firestein, S. (2009). Ablation of mouse adult neurogenesis alters olfactory bulb structure and olfactory fear conditioning. *Frontiers in Neuroscience*, *3*. doi:10.3389/neuro.22.003.2009

Wang, C., Liu, F., Liu, Y.-Y., Zhao, C.-H., You, Y., Wang, L., Zhang, J., Wei, B., Ma, T., Zhang, Q., Zhang, Y., Chen, R., Song, H., & Yang, Z. (2011). Identification and characterization of neuroblasts in the subventricular zone and rostral migratory stream of the adult human brain. *Cell Research*, *21*(11), Article 11. doi:10.1038/cr.2011.83

Wang, D., Liu, P., Mao, X., Zhou, Z., Cao, T., Xu, J., Sun, C., & Li, A. (2019). Task-Demand-Dependent Neural Representation of Odor Information in the Olfactory Bulb and Posterior Piriform Cortex. *Journal of Neuroscience*, *39*(50), 10002–10018. doi:10.1523/JNEUROSCI.1234-19.2019

Wang, S., Tan, N., Zhu, X., Yao, M., Wang, Y., Zhang, X., & Xu, Z. (2018). Sh3rf2 Haploinsufficiency Leads to Unilateral Neuronal Development

Deficits and Autistic-Like Behaviors in Mice. *Cell Reports*, *25*(11), 2963-2971.e6. doi:10.1016/j.celrep.2018.11.044

Wegscheid, M. L., Anastasaki, C., Hartigan, K. A., Cobb, O. M., Papke, J. B., Traber, J. N., Morris, S. M., & Gutmann, D. H. (2021). Patient-derived iPSC-cerebral organoid modeling of the 17q11.2 microdeletion syndrome establishes CRLF3 as a critical regulator of neurogenesis. *Cell Reports*, *36*(1). doi:10.1016/j.celrep.2021.109315

Wesson, D. W., Levy, E., Nixon, R. A., & Wilson, D. A. (2010). Olfactory Dysfunction Correlates with Amyloid-β Burden in an Alzheimer's Disease Mouse Model. *Journal of Neuroscience*, *30*(2), 505–514. doi:10.1523/JNEUROSCI.4622-09.2010

Xu, H., Geng, C., Hua, X., Liu, P., Xu, J., & Li, A. (2021). Distinct Characteristics of Odor-evoked Calcium and Electrophysiological Signals in Mitral/Tufted Cells in the Mouse Olfactory Bulb. *Neuroscience Bulletin*, *37*(7), 959–972. doi:10.1007/s12264-021-00680-1

Yamada, Y., Bhaukaurally, K., Madarász, T. J., Pouget, A., Rodriguez, I., & Carleton, A. (2017). Context- and Output Layer-Dependent Long-Term Ensemble Plasticity in a Sensory Circuit. *Neuron*, *93*(5), 1198-1212.e5. doi:10.1016/j.neuron.2017.02.006

Zhao, Z., Xing, J., Zhang, X., Qu, X., Hu, X., & Lu, J. (2022). Random and Short-Term Excessive Eye Movement in Children with Autism During Face-to-Face Conversation. *Journal of Autism and Developmental Disorders*, *52*(8), 3699–3710. doi:10.1007/s10803-021-05255-7

국문초록

성체후각신경생성 조절을 통한 생쥐 정서식별에서 NEGR1의 역할

정서인식과 감각반응성은 자폐스펙트럼장애(ASD) 환자에서 주로 손상된다. 정서적 정보는 표정, 말투, 체취와 같은 감각적 정보를 통해 전달된다. ASD 환자들의 비정형적 감각 민감성을 고려할 때 조절되지 않는 사회정서적 감각 정보가 정서인식 장애로 이어질 수 있음을 알 수 있다. 하지만, 아직까지 자폐 생쥐 모델에서 정서인식 장애의 유무가 연구되지 않아 ASD의 정서인식과 감각정보처리 간 관계를 탐구하는데 어려움이 있다. 이 연구에서는 neuronal growth regulator 1 (*Negr1*) 결손 생쥐를 이용해 정서식별과 후각 정보처리과정에 대한 NEGR1의 기능을 조사하였다. *Negr1* 결손 생쥐는 정상 생쥐와 달리 속박 스트레스나 만성통증을 느끼는 상대 쥐와 정서적으로 중립적인 쥐가 함께 놓였을 때 선택적인 사회적 탐색 행동을 보이지 못하며 정상적인 정서 식별을 수행하지 못하였다. 더욱이 *Negr1* 결손 생쥐는 사회적 냄새에 대한 탐지능력에는 문제가 보이지 않았음에도 불구하고 사회적 냄새에 대한 비정상적인 후각 습관화와 탈습관화를 보였다. 전기생리학적으로는 후각망울(olfactory bulb) 내 승모세포(mitral cell)에 대한 억제신호가 *Negr1* 결손 생쥐에서 증가되어 있고, 이어 세포의 흥분성은 감소되어 있었다. 이에 대한 기제로서 *Negr1* 결손 생쥐의 후하부뇌실질(posterior subventricular zone) 내 성체신경생성(adult neurognesis)에 손상이 있으며 이는 후각망울 내 신생억제뉴런의 수 감소로 이어졌다. 종합적으로 이 결과들은 NEGR1에 의해 매개되는 정서인지와 후각신호처리 간 관련성을 밝히고 있으며 손상된 성체후각신경생성에 따른 자폐 관련 행동들의 새로운 신경생물학적 기제를 제안한다.

주요어: Neuronal growth regulator 1 (NEGR1); 자폐증; 정서식별; 후각 정보처리; 성체후각신경생성

학번: 2020-22323

ACKNOWLEDGEMENT

학위 논문을 마무리 하며 가장 먼저 과학적 소양을 바닥부터 길러 주신 이성중 지도 교수님께 감사드립니다. 교수님께서 랩 미팅 중 어느 날 '과학은 눈금자의 눈금을 더 작게 나누어 가는 과정이다.'라며 말씀해주신 것을 기억합니다. 석사 과정과 실험, 그리고 논문 작성의 과정 동안 교수님의 이 말씀은 제 스스로 눈금을 쪼개 가고 있는지 돌아보게 하였습니다. 단순히 과학적 기술과 지식을 늘리는 것에 그치는 것이 아닌 과학자로서 태도와 의식까지 길러 주신 이성중 교수님께 감사드립니다.

이 논문을 작성함에 있어 많은 도움을 준 우리 연구실 동료들께 감사드립니다. 그 중에서도 자신의 노하우와 경험을 아낌없이 나누어 준 노경철 박사님과 시작을 함께하여 지금까지 연구와 과학에 대해 끊임 없이 같이 나누며 성장하고 있는 황민규 학생, 그리고 팀 동료인 조우현 박사님과 Dr. Ellane Barcelon에게 감사드립니다.

지난 석사 과정 동안 뇌인지과학을 배울 수 있도록 환경을 만들어 주시고 관심 가져 주신 이인아 교수님과 이상아 교수님께 진심으로 감사드립니다. 뇌인지 과학이 한국에서 꽃 피우길 바라며 기꺼이 헌신해주신 마음을 많이 느낄 수 있었습니다, 학과 행사나 교과목 등에서 뇌인지과학에 대한 교수님들의 통찰과 시선을 배웠습니다. 교수님들께 학위 논문 심사를 받을 수 있어 영광이라는 말씀을 드리고 싶습니다.

또한 일반에 순응하지 않고 예측 불가능하며 불안한 삶을 이어가는 저를 언제나 사랑으로 지지해주고 기다려주며 응원해주는 가족에게 감사드립니다. 몇 년의 학위 과정이었고, 몇 달의 학위 논문 작성이었지만, 평생에 걸친 부모님과 동생의 애정이 없었다면 지금의 저는 없었을 것입니다. 먼 발치에서 언제나 저를 자랑스럽게 여겨 주시어 감사드립니다.

마지막으로 모든 행복의 순간에 옆에서 함께 있어 주는 가경이에게 고맙다는 말을 전하고 싶습니다. 그녀의 따뜻함과 웃음 소리가 제 의지의 양식이 되어 힘을 낼 수 있었습니다. 나의 이유가 되어 주어 고맙습니다. 끝마치며 한 치 앞을 알 수 없는 제 인생을 언제나 선한 것으로 채워 주신 하나님께 감사드립니다.